1 Langmuir probe diagnostics of low-temperature plasmas

Sigismund Pfau[†] *and Milan Tichý*[‡]

[†] Institut für Physik, Ernst-Moritz-Arndt-Universität Greifswald, Domstraße 10a, D-17487 Greifswald, Germany
[‡] Charles University in Prague, Faculty of Mathematics and Physics, Department of Electronics and Vacuum Physics, V Holešovičkách 2, 18000 Praha 8, Czech Republic

1.1 Introduction

1.1.1 Probe shapes and probe characteristics

Measurements with electric probes belong to the oldest as well as to the most often used procedures of the low-temperature plasma diagnostics. The method has been developed by Langmuir and his co-workers in the twenties [1]. Since then it has been subject of many extensions and of further developments in order to extend its applicability to problems with more general conditions as those presumed by Langmuir. Such investigations proceeded continuously and the research on extension of applicability of Langmuir probe diagnostics continues in the present time, too.

The method of the Langmuir probe measurements is based on the estimation of the current-voltage characteristics – the so-called *probe characteristics* – of a circuit consisting of two metallic electrodes that are both immersed into the plasma under study. Two cases are of interest:

(a) the surface areas of both the electrodes being in contact with plasma differ by several orders of magnitude, and

(b) the surface areas of both the electrodes being in contact with plasma are very small in comparison with the dimensions of the vessel containing plasma and approximately equal to each other.

Case (a) is called *the single probe method*, case (b) *the double probe method*. Most of this text is devoted, in accordance with the frequency of use of either method, to the single probe method; the double probe method is discussed in section 1.10.

The Langmuir probe is usually constructed in simple geometric shapes: spherical probe, cylindrical probe and planar (flat) probe, see Fig. 1.1. When constructing the probe we have to take into account that not only the active metallic part, i.e., the collecting surface of the probe, has to be small in comparison with the characteristic dimensions of the plasma vessel. The isolated parts of the probe must fulfill the same condition since often just these passive parts substantially influence the plasma around the probe .

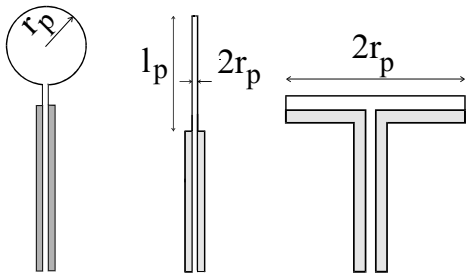

Figure 1.1: Typical shapes of Langmuir probes .

A simple experimental set-up for measurements of probe characteristics is shown in Fig. 1.2. Apart from the direct current (*dc*) high-voltage power supply that feeds the glow discharge and the stabilizing resistor Z_a (the *dc* supply can also work in the constant-current mode) the experimental system consists of the following parts:

1. a *dc* voltage source for compensation of the potential difference between the reference electrode (anode) and the probe,
2. a sawtooth- or staircase-like voltage generator,
3. a current measuring instrument, and
4. a computer that stores the measured current and voltage data, controls the measurement procedure and processes the acquired data.

Let us assume that the probe potential φ_p differs from the plasma (space) potential φ_s at the place where the probe is located by $U_p = \varphi_p - \varphi_s \neq 0$. In such a case the electric field that arises between the plasma and the probe surface accelerates the charged particles with one sign

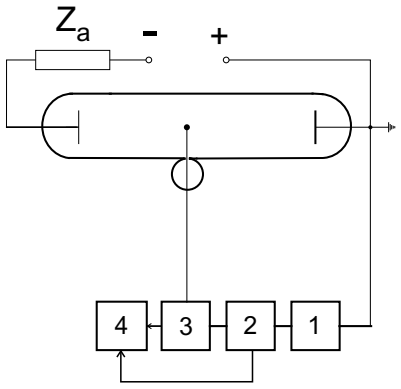

Figure 1.2: Typical probe circuit. 1 *dc* bias voltage, 2 sawtooth or staircase U_p generator, 3 current–voltage converter, 4 $I_p - U_p$ data acquisition (computer).

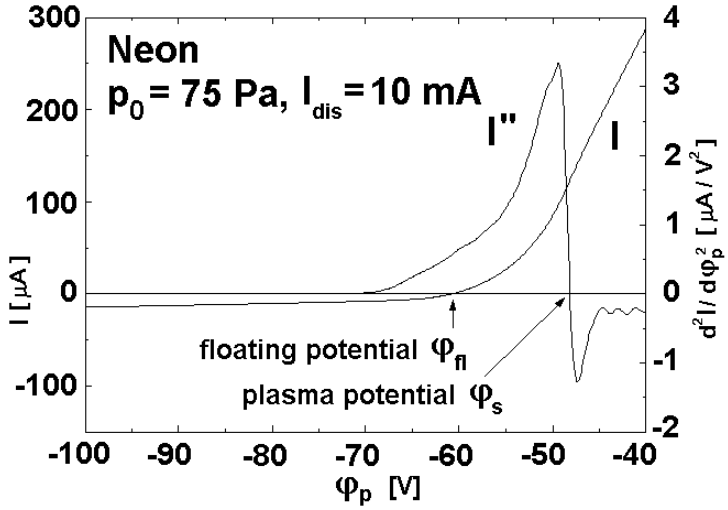

Figure 1.3: Typical course of the probe characteristics $I(\varphi_p)$ (left scale) with its second derivative $I'' \equiv d^2I/d\varphi_p^2$ (right scale).

and repels those with the opposite sign. Since the charged particles have thermal energy that randomizes their movement this process finishes with the creation of a space charge sheath around the probe which shields the plasma from the electric field of the probe. A simplified physical model of such a probe assumes that the space charge sheath has a finite thickness. This means that the influence of the electric field extends only up to a certain distance from the probe and that the plasma farther away from the probe is perfectly shielded. The thickness of the probe sheath ($r_p - r_s$) is of the order of the so-called Debye length (λ_D). The Debye length for the electrons can be obtained from the well known formula (see also chapter **??**)

$$\lambda_D \;=\; \sqrt{\frac{\varepsilon_0 k_B T_e}{q_0^2 n_e}}\,, \tag{1.1}$$

where T_e is the electron temperature, n_e the concentration of the electrons, ε_0 the permittivity of the vacuum, k_B the Boltzmann constant, and q_0 the elementary charge. The thickness of the probe sheath at moderate U_p actually is several times λ_D and increases with increasing U_p. If the potential of the probe surface is changed with respect to the space potential the probe current changes too, and finally the probe characteristics will be obtained. A typical course of the probe characteristics is shown in Fig. 1.3.

Three regions can be clearly distinguished in the course of the probe characteristics. Assuming that no negative ions exist in the plasma the probe current consists of the electron and the positive ion current. The three regions of the probe characteristics are characterized by:

I.	$U_p \leq 2U_{fl}$	$\rightarrow$	$\mid I_{pi}/I_{pe} \mid$	$\gg$ 1	Positive ion acceleration region
II.	$2U_{fl} < U_p < 0$	$\rightarrow$	$\mid I_{pi}/I_{pe} \mid$	$\approx$ 1	Transition region
III.	$0 \leq U_p$	$\rightarrow$	$\mid I_{pi}/I_{pe} \mid$	$\ll$ 1	Electron acceleration region

In the ion acceleration region (sometimes called ion saturation region since the ion current is close to saturation) an almost pure positive ion current flows to the probe. At the floating potential the electron and the positive ion current compensate each other and the total probe current equals to zero. For positive probe voltages the electron current dominates the probe current; the probe operates in the electron acceleration region. If the probe immersed into plasma is not connected to the outer circuit, and therefore it cannot carry the current, then the probe is negatively charged with respect to the plasma potential. This takes place since the electrons (even at the same temperature like positive ions) have a much higher thermal velocity due to their much lower mass (typically for argon is the square root of the mass ratio around 300). The more negative potential of the probe, in consequence, attracts more positive ions, and this process continues until the electron and the positive ion current components equal each other; the floating potential is established on the probe.

The contact of the plasma and the probe surface, i.e. the contact of two basic states of aggregation of matter causes the creation of a largely inhomogeneous transition region close to the probe surface which is very difficult to describe. Characteristic for this transition region are the space charges and high electric fields. The theoretical description of this region is coupled with substantial difficulties.

With the help of a theoretical description of the relation between the probe current and the probe voltage it is possible to determine the basic parameters of the surrounding plasma. In such a way we can determine the density of the electrons n_e and of the positive ions n_i, the electron temperature T_e or the electron velocity (energy) distribution function $f_e(\vec{w}, \vec{r})$ as well as the space potential at the place where the probe is located. The theory of the probe method will actually be confronted with all the problems connected with the contact between plasma and solid surface. The importance of the probe theory therefore reaches far behind the borders of probe diagnostics.

1.1.2 The working regimes of the Langmuir probe

In order to characterize the different regimes of operation of the Langmuir probe we introduce the following parameters:

- the characteristic dimension r_p of the probe,
- the mean free path λ_ν of a particular charged particle $\nu = e, i$ (e, electron; i, ion),
- the Debye screening length λ_D (Eq. 1.1), and
- the plasma *anisothermicity parameter* $\tau = T_e/T_i$, i.e. the ratio of the electron temperature to the ion temperature.

The following part restricts at first to the presentation of the theoretical foundations of the *classic* Langmuir *collisionless* single probe theory. The adjective *collisionless* represents the assumption posed by Langmuir that the mean free path of charged particles is much greater than the characteristic dimension of the probe: $\lambda_\nu \gg r_p$. Assuming this three working regimes of the probe we have to distinguish:

1. $\lambda_\nu \gg r_p \gg \lambda_D$ collisionless movement of charge carriers in the thin sheath,
2. $\lambda_\nu \gg \lambda_D \gg r_p$ collisionless movement of charge carriers in the thick sheath,
3. $\lambda_D \gg \lambda_\nu \gg r_p$ collision determined description of the probe current.

The case of the so-called *continuum probe* working regime, when the condition $\lambda_\nu \ll r_p$ is fulfilled, shall not be discussed here.

1.1.3 Advantages and disadvantages of probe diagnostics

The most important advantages of probe diagnostics in comparison to other diagnostic methods can be found in the following attributes:

- The technical complexity of the probe method implementation is comparatively small. Also, the necessary experimental set-up for the probe measurements is comparatively simple.
- From the probe data it is possible to determine the time and spatial distribution of quite a large variety of quantities characterizing the plasma under study (i.e., n_e, n_i, T_e, f_e, φ_s, $\vec{E}$, etc.).

The spatial resolution of the probe method is of the order of the magnitude of the Debye length λ_D. The temporal resolution may be estimated from the plasma frequency ω of a charged particle with mass m

$$\omega = \sqrt{\frac{q_0^2 n_i}{\varepsilon_0 m}}\,, \tag{1.2}$$

it is approximately given by $2\pi/\omega_i$, where $\omega = \omega_i$ is the plasma frequency for an ion of mass $m = m_i$.

The disadvantages of the probe method are the following:

- The probe data processing method (aiming at the determination of the plasma parameters) depends on the parameters being measured.
- The plasma surrounding the probe is disturbed by the drain of the charge carriers to the probe.
- The presence of the probe in the plasma can initiate inhomogeneities in the plasma.
- The application of the probe method is difficult or even impossible in a plasma containing fluctuations, oscillations and waves.

- It is very difficult to assess the effect of the secondary- and photo-emission of electrons from the probe surface as well as the effect of reflection of charge carriers from the probe surface.

- The heavy particles can cause the creation/destruction of thin films on the probe surface during the course of measurements which change the properties of the probe surface, this making the interpretation of the probe data difficult or impossible.

- The fact that the probe is in direct contact with the plasma under study restricts its use substantially to the (non-thermal or thermal) low-temperature plasma. The use of probes for the diagnostics of plasma in high-temperature plasma devices such as tokamaks is restricted to peripheral parts of the plasma, the so-called scrape-off layer (SOL).

1.2 The Langmuir single probe method

1.2.1 Theoretical foundations of the Langmuir probe method

The range of the conventional Langmuir probe theory covers the conditions of the collisionless movement of charge carriers in the space charge sheath around the probe. Further it is assumed that the sheath boundary is well-defined and that behind this boundary the plasma is completely undisturbed by the presence of the probe. This means that the electric field caused by the difference between the potential of the probe and the plasma potential at the place where the probe is located is limited to the volume inside the probe sheath boundary and does not penetrate it.

Assuming that the velocity distribution function f_ν of a charged particle ν ($\nu = e, i$) at the surface area of the probe sheath is known, we can obtain the following expression for the number of charged particles passing the surface area element dA_s of the sheath boundary per unit of time:

$$dI_{\nu s} \;=\; dA_s dj_{\nu s} \;=\; dA_s q_\nu n_\nu w_z f_\nu(w_x, w_y, w_z) dw_x dw_y dw_z \,. \tag{1.3}$$

Here q_ν is the charge and n_ν the density of the charged particle ν, $j_{\nu s}$ its current density at the sheath boundary, and w_z, w_x and w_y are the velocity vector components perpendicular respectively parallel to the surface area element dA_s. If the distribution function f_ν is isotropic and the surface A_s is not concave, then the contribution of each surface element is independent of its orientation in space. In such a case the total current can be obtained by simple integration over the surface elements dA_s.

For a certain probe potential the fraction of particles that fall on the probe surface without passing it can be determined by the choice of proper integration limits. In general we have

$$I_{p\nu} \;=\; A_s q_\nu n_\nu \int_{w_{x1}}^{w_{x2}} \int_{w_{y1}}^{w_{y2}} \int_{w_{z1}}^{w_{z2}} w_z f_\nu(w_x,\; w_y,\; w_z)\; dw_x dw_y dw_z \,. \tag{1.4}$$

In the case of the spherical probe it is advantageous to transform the cartesian velocity coor-

dinates w_x, w_y, w_z into spherical coordinates w, ϑ, φ,

$$I_{p\nu} \;=\; \frac{A_s q_\nu n_\nu}{4} \int_{w_1}^{w_2} 4\pi w^3 \; f_\nu(w) \left[\sin^2 \;\vartheta_2 - \sin^2 \;\vartheta_1\right] dw \,. \tag{1.5}$$

1.2.2 Probe characteristics – example of the spherical probe

1.2.2.1 Probe current at $q_\nu U_p \geq 0$

As an example for the calculation of the current to a Langmuir probe the case of a spherical probe shall be examined. Fig. 1.4 enlightens the movement of a charged particle in the retarding field (i.e., for $q_\nu U_p \geq 0$) of a spherical probe. where ϑ is the incident angle of

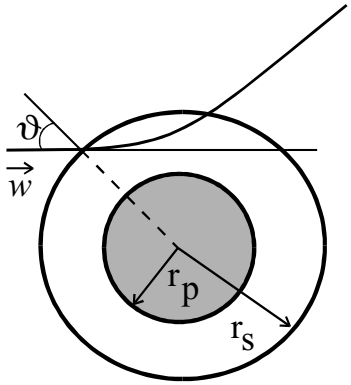

Figure 1.4: Model trajectory.

the particle with respect to the surface normal, $\vec{w}$ its incident velocity into the space charge sheath, and r_p and r_s are the probe and sheath radii, respectively. It is assumed that a particle that enters the space charge sheath moves collision-free in the central field of the probe. Its movement is then governed by two laws of conservation, namely that of energy and that of angular momentum. For the particles that fall on the probe surface the condition

$$\sin\vartheta \leq \frac{r_p}{r_s}\left(1 - \frac{2q_\nu U_p}{m_\nu w^2}\right)^{\frac{1}{2}} \tag{1.6}$$

holds, from which the following limits of integration can be derived

$$\vartheta_1 \;=\; 0 \qquad \text{and} \qquad \sin\vartheta_2 \;=\; \frac{r_p}{r_s}\left(1 - \frac{2q_\nu U_p}{m_\nu w^2}\right)^{\frac{1}{2}} \;\geq 0 \tag{1.7}$$

and

$$w_1 \;=\; \left(\frac{2q_\nu U_p}{m_\nu}\right)^{\frac{1}{2}} \qquad \text{and} \qquad w_2 \;=\; \infty \,. \tag{1.8}$$

Hence the probe current $I_{p\nu}$ of the particle ν is obtained by the integral

$$I_{p\nu} \;=\; \frac{A_s q_\nu n_\nu}{4} \int\limits_{\sqrt{\frac{2q_\nu U_p}{m_\nu}}}^{\infty} 4\pi w^3 f_\nu(w) \left(\frac{r_p}{r_s}\right)^2 \left[1 \;-\; \frac{2q_\nu U_p}{m_\nu w^2}\right] dw\,. \tag{1.9}$$

Assuming that the velocity distribution of the charged particle ν is Maxwellian this relation after a few manipulations can be simplified to

$$I_{p\nu} \;=\; \frac{A_p q_\nu n_\nu}{4}\; \overline{w}_\nu \;\exp\left(-\frac{q_\nu U_p}{k_B T_\nu}\right), \tag{1.10}$$

where

$$\overline{w}_\nu \;=\; \left(\frac{8k_B T_\nu}{\pi m_\nu}\right)^{\frac{1}{2}} \tag{1.11}$$

and $A_p = 4\pi r_p^2$. The same equation is obtained for the planar probe and for the cylindrical probe (in these cases A_p denotes the surface area of the collecting probe plane or cylinder, respectively).

The temperature T_ν of the charged particles ν is obtained from the derivative (slope) of the probe characteristics in the respective retarding voltage range on a semi-logarithmic scale, i.e., as

$$T_\nu \;=\; -\frac{q_\nu}{k_B}\frac{d}{dU_p}\ln\left(\frac{I_{p\nu}}{I_{p\nu 0}}\right). \tag{1.12}$$

The charged particle density n_ν can be estimated from the probe current $I_{p\nu 0}$ at the space potential ($U_p = 0$), provided the space potential is known and that it is possible to separate the current contribution of the particle ν from the total probe current. The corresponding relation obtained from Eq. 1.10 is

$$I_{p\nu 0} \;=\; A_p q_\nu \frac{n_\nu}{4}\; \overline{w}_\nu \tag{1.13}$$

from which n_ν is obtained as

$$n_\nu \;=\; \frac{4I_{p\nu 0}}{A_p q_\nu \overline{w}_\nu}\,. \tag{1.14}$$

We have to keep in mind, however, that we only are able to measure the total probe current. In the transition region II (see section 1.1.1) between the positive ion acceleration region I and the electron acceleration region III both, electron and positive ion current, are comparable to each other. In order to separate these contributions from each other one can use several procedures, e.g., one can extrapolate the *saturated* positive ion current to the space potential in a linear manner and subtract this positive ion current component from the total probe current. ¿From this consideration it also follows that only for electrons it is possible to estimate the particle temperature T_ν from the relation 1.12, but not for ions except under very special operating conditions.

1.2.2.2 Probe current at $q_\nu U_p \leq 0$

In a manner similar to the procedure above we can derive, for $q_\nu U_p \leq 0$ and with the help of the energy and angular momentum conservation laws, the integration limits for ϑ and w for particles which fall on the probe surface at a given probe potential. In analogy to Eqs. 1.7 and 1.8 we get

$$\vartheta_1 \;=\; 0 \qquad \text{and} \qquad \sin\vartheta_2 \;=\; \frac{r_p}{r_s}\left(1-\frac{2q_\nu U_p}{m_\nu w^2}\right)^{\frac{1}{2}} \leq 1\,. \tag{1.15}$$

With the collected particle velocities now in the range $w_1 = 0$ to $\omega_2 = \infty$ we can distinguish 2 cases: for $0 \leq w \leq w^*$ we get $\sin\vartheta_2 = 1$, while for $w \geq w^*$ expression 1.15 holds. By substituting these limits into equation 1.5 for the probe current we obtain

$$I_{p\nu} = \frac{A_s n_\nu q_\nu}{4}\left\{\int_0^{w^*} 4\pi w^3 f_\nu(w)dw + \int_{w^*}^{\infty} 4\pi w^3 f_\nu(w)\frac{r_p^2}{r_s^2}\left(1-\frac{2q_\nu U_p}{m_\nu w^2}\right)^2 dw\right\}\,, \tag{1.16}$$

where

$$w^* = \left\{-2q_\nu U_p/m_\nu\left[r_s^2/r_p^2\;-1\right]\right\}^{\frac{1}{2}}\;. \tag{1.17}$$

For the velocity interval $0 \leq w \leq w^*$ the probe acts as a collector with an effective collecting area that is larger than the true surface area A_p of the probe. For charged particle velocities $w \geq w^*$ a part of the charged particles which entered the probe sheath passes by the probe and is not collected by the probe (so-called orbital motion limited current, OML). Assuming a Maxwellian velocity distribution $f_\nu(w)$ we obtain from (1.16)

$$I_{p_\nu} \;=\; \frac{n_\nu}{4} q_\nu \overline{w}_\nu A_s\left[1-\left(1-\frac{r_p^2}{r_s^2}\right)\exp\left(\frac{q_\nu U_p}{k_B T_\nu\left(\frac{r_s^2}{r_p^2}-1\right)}\right)\right]\;. \tag{1.18}$$

On condition that

$$-\frac{k_B T_\nu}{q_\nu U_p}\left(\frac{r_s^2}{r_p^2}-1\right) \gg 1 \tag{1.19}$$

we get from the above relation

$$I_{p_\nu}^{(s)} \;=\; q_\nu \frac{n_\nu}{4}\overline{w}_\nu A_p\left\{1-\frac{q_\nu U_p}{k_B T_\nu}\right\} \tag{1.20}$$

for the spherical probe, and

$$I_{p_\nu}^{(c)} \;=\; q_\nu \frac{n_\nu}{4}\overline{w}_\nu A_p\left\{1-\frac{q_\nu U_p}{k_B T_\nu}\right\}^{\frac{1}{2}} \tag{1.21}$$

for the cylindrical probe. For the planar probe we obtain a current that is independent of the probe potential,

$$I_{p_\nu}^{(p)} \;=\; q_\nu \frac{n_\nu}{4}\overline{w}_\nu A_p\,. \tag{1.22}$$

While the evaluation of the relations 1.20–1.22 provides usable results for electrons, this does not hold for ions. A more detailed analysis of the transition region between the undisturbed

non-thermal plasma and the region of the space charge sheath was performed by Bohm [2]. He showed that the sheath screens the electric field from the probe imperfectly, i.e., a *rest* potential $k_B T_e/(2q_0)$ (Bohm criterion) remains. This *rest* potential is screened by the so-called pre-sheath that spans from the probe sheath to infinite distance. For this reason the positive ions entering the probe sheath do not have room temperature as in an undisturbed plasma, but are accelerated in the pre-sheath, their temperature being determined by the temperature of the electrons.

1.3 General theories of the current to a Langmuir probe

1.3.1 Starting system of equations

The general theoretical description of the current to a Langmuir probe requires the simultaneous solution of the following fundamental equations

- the Poisson equation
- the collision-free Boltzmann (Vlasov) equation and
- the continuity equation

with regard to the respective boundary conditions at the probe surface and in the plasma. At a larger distance from the probe such solution must be identical to the solution which corresponds to the undisturbed plasma. At the probe surface the boundary conditions are determined by complex processes of the plasma-wall interaction. The starting system of equations reads:

$$\mathrm{div}\vec{E} \;=\; \frac{q_0}{\varepsilon}(n_i - n_e)\,, \tag{1.23}$$

$$\vec{w}_\nu \mathrm{grad} f_\nu \;+\; \frac{q_\nu}{m_\nu}\vec{E}\,\mathrm{grad}_w f_\nu \;=\; 0\,, \tag{1.24}$$

$$\mathrm{div}(\vec{j}_e \;+\; \vec{j}_i) \;=\; 0 \tag{1.25}$$

with the normalizing conditions

$$\int_{-\infty}^{+\infty}\int_{-\infty}^{+\infty}\int_{-\infty}^{+\infty} f_\nu(w_x, w_y, w_z)dw_x dw_y dw_z \;=\; n_\nu\,; \qquad \nu \;=\; i, e\,. \tag{1.26}$$

The simultaneous solution of this set of equations presents a very complicated problem which can be solved only numerically and by using substantial computational effort. If the method of solution takes into account the redistribution of charges induced by the change of the probe potential and consequently of the probe current, such a solution is called self-consistent. Such a self-consistent solution of this integro-differential system of equations was firstly stated by Bernstein and Rabinowitz under the assumption of a monoenergetic ion energy distribution [3]. This solution was developed further by Laframboise who assumed a Maxwellian ion energy distribution [4]. A simplified model for the calculation of the ion current was developed by Allen, Boyd and Reynolds [5]. Since this model is one of the most often used theories for the interpretation of the probe data it shall be explained in more detail in the following section.

1.3.2 The *cold ion* model by Allen, Boyd and Reynolds ($T_i/T_e = 0$)

The starting system of equations of this model [5] consists of the Poisson equation, the simplified ion energy balance, the Boltzmann distribution of the electron density and the continuity equation. Assuming spherical symmetry such a system of equations can be written as:

$$\text{Poisson equation :} \qquad \frac{1}{r^2}\frac{d}{dr}\left(r^2\frac{dU}{dr}\right) = -\frac{q_0}{\varepsilon}(n_i - n_e)\,, \tag{1.27}$$

$$\text{ion energy balance :} \qquad \frac{1}{2}m_i w_r^2 = -q_0 U\,, \tag{1.28}$$

$$\text{Boltzmann distribution :} \qquad n_e = n_{e0}\exp\left(\frac{q_0 U}{k_B T_e}\right)\,, \tag{1.29}$$

$$\text{continuity equation :} \qquad \frac{1}{r^2}\frac{d}{dr}(r^2 j_{ir}) = 0 \quad \text{with} \quad 4\pi r^2 j_{ir} = I_{pi}\,. \tag{1.30}$$

It is usual to introduce dimension-less variables, i.e., variables that are normalized with respect to *reasonable* or *representative* values of each variable. Allen, Boyd and Reynolds [5] introduced the normalized variables as follows:

$$\eta = \frac{q_0 U}{k_B T_e} \quad ; \qquad \eta_p = \frac{q_0 U_p}{k_B T_e}\,; \tag{1.31}$$

$$\xi = \frac{r}{\lambda_D} \quad ; \qquad \xi_p = \frac{r_p}{\lambda_D}\,; \tag{1.32}$$

$$i_i = \frac{I_{p_i}}{I_{n_i}} \quad ; \qquad I_{n_i} = 4\pi r_p^2 n_{e0} q_0 \left\{\frac{k_B T_e}{2\pi m_i}\right\}^{\frac{1}{2}}\,. \tag{1.33}$$

Using these variables the Poisson equation 1.27 reads

$$\frac{d}{d\xi}\left(\xi^2\frac{d\eta}{d\xi}\right) = \xi^2\exp(\eta) - \xi_p\frac{i_i}{2\sqrt{-\pi\eta}}\,. \tag{1.34}$$

The solution of this equation proceeds in such a way that for large ξ it converges to the so-called plasma solution. The plasma solution is obtained by setting the left-hand side of the equation 1.34 equal to zero. For $\eta \to -\frac{1}{2}$ the derivative increases to infinity, $\frac{d\eta}{d\xi} \to \infty$. This result is known as the Bohm sheath criterion [2]. From the solution of the differential equation

$$\eta = \eta(\xi, \xi_p, i_i) \tag{1.35}$$

follows the mutual relation between the three quantities η_p, ξ_p and i_i. The results are available in the form of tables, graphical representations and analytical approximations. In the following section the method of estimation of the positive ion density from the ion probe current on the basis of the described cold ion model by Allen, Boyd and Reynolds shall shortly be outlined. Since the normalized ion current i_i depends on ξ_p which in turn depends on the ion density to be estimated the first possibility is the iterative procedure. For the selected pair of values I_{pi} and η_p (in other words the electron temperature has to be determined first) on the measured probe characteristics we have to estimate (the first approximation of) $\xi_p^{(1)}$. From the dependence $i_i = i_i(\xi_p, \eta_p)$ then it is possible to estimate the normalized current $i_i^{(1)}$. Since I_{pi} is already known it is possible to determine the $I_{ni}^{(1)}$ from equation 1.33 and hence the first

approximation of the ion density $n_i^{(1)}$. From this density value the second order approximation of $\xi_p^{(2)}$ is calculated, etc., until the approximations $n_i^{(k-1)}$ and $n_i^{(k)}$ do not differ *too much* from each other. The convergence of this procedure is unclear and depends very much on the first choice of $\xi_p^{(1)}$.

The necessity of the iterative procedure was removed by Sonin by introducing the so-called *Sonin plot* [6]. This plot relates the artificially created quantity $\xi_p^2 i_i$ to i_i at a pre-selected value of η_p, usually $\eta_p = \eta_{fl} - 10$ [21] or $\eta_p = -15$ [18]. Since ξ_p^2 is proportional to n_i and i_i is inversely proportional to n_i the quantity $\xi_p^2 i_i$ does not depend on n_i and hence excludes the necessity of the iterative procedure

$$\xi_p{}^2 i_i \;=\; \frac{1}{\varepsilon}\left\{\frac{m_i}{8\pi q_0}\right\}^{\frac{1}{2}}\left(\frac{q_0}{k_B T_e}\right)^{\frac{3}{2}}\; I_{p_i}\;. \tag{1.36}$$

Analytical approximations of the relation $i_i = i_i(\xi_p, \eta_p)$ are available for the spherical as well as for the cylindrical probe. For example, the approximation for the cylindrical probe can be written as [7]

$$i_i(\eta_p) \;=\; a(\eta_p/b)^{\alpha}\,, \tag{1.37}$$

where

$$a \;=\; (\xi_p + 0.6)^{0.05} + 0.04\,, \quad b = 0.09\,\left(\exp(-\xi_p^{-1}) + 0.08\right)\,, \tag{1.38}$$

$$\alpha \;=\; (\xi_p + 3.1)^{-0.6}\,. \tag{1.39}$$

The radial motion theory has been further developed and tested. The relevant publications are [8] (application of the radial motion theory in a radiofrequency (*rf*) discharge in argon), [9] (review on OML theories, recent experimental work), [10] (new modern aspects together with recent developments in experimental techniques), [11] (extension for double probe), and [12] (small body floating in a plasma). Further the radial motion theory has been extended to the interesting case of the so-called standard electron energy distributions [13], i.e.,

$$f^*(u_p) = \text{const.} \times \varepsilon_p^{-3/2} \exp\left(-\frac{u_p^k}{k\varepsilon_p^k}\right) \qquad \text{with } k \geq 1\,. \tag{1.40}$$

Here u_p represents the voltage equivalent of the electron energy (see the paragraph below) and ε_p is the so-called effective electron temperature. For $k = 1$ this distribution represents the Maxwellian, for $k = 2$ the Druyvesteynian, and for $k = 4$ the Davydov distribution (see also chapter **??**). The case of finite ion temperature values, i.e. of arbitrary ratios T_i/T_e has been treated in Ref. [14]. This theory includes the classical ABR theory (developed for $T_i/T_e \to 0$) as a special case.

1.4 The Druyvesteyn method for estimation of the electron energy distribution function (EEDF)

One of a few procedures that permit the direct experimental determination of the electron energy distribution function EEDF in a plasma is based on the probe measurements. In order

to explain this procedure the investigation starts at the probe characteristics in the electron retarding region given by equation 1.9. In order to express the variables in terms of energy the quantities q_ν, U_p and w are substituted by $-q_\nu = q_0, -U_p = u_p$ and $w = (2q_0u/m_e)^{1/2}$. Then by differentiating equation 1.9 with respect to u at the point $u = u_p$ the well-known Druyvesteyn relation follows [15]:

$$\frac{d^2 I_{p_e}}{du_p^2} \;=\; \left(\frac{q_0}{2}\right)^{\frac{3}{2}} m_e^{-\frac{1}{2}} n_e A_p \overline{f}(u_p)\,, \tag{1.41}$$

where $\overline{f}(u_p)$ fulfills the normalizing condition

$$\int_0^\infty \overline{f}(u_p)\; u_p^{\frac{1}{2}}\; du_p \;=\; 1\,. \tag{1.42}$$

Eq. 1.41 enables us to estimate the electron density n_e and the mean electron energy q_0u_m using the relations

$$n_e \;=\; \left(\frac{2}{q_0}\right)^{\frac{3}{2}} \frac{m_e^{\frac{1}{2}}}{A_p} \int_0^\infty u_p^{\frac{1}{2}} \frac{d^2 I_{p_e}}{du_p^2} du_p \tag{1.43}$$

and

$$q_0 u_m \;=\; \frac{q_0 \int\limits_0^\infty u_p^{\frac{3}{2}} \frac{d^2 I_{p_e}}{du_p^2}\; du_p}{\int\limits_0^\infty u_p^{\frac{1}{2}} \frac{d^2 I_{p_e}}{du_p^2}\; du_p}\,. \tag{1.44}$$

It is very important to fix the origin of the energy scale for the EEDF, in other words to determine the space (plasma) potential at the probe position. In accordance with the works of Luijendijk and van Eck [16] and Herrmann and Klagge [17] the space potential is most accurately determined as the probe voltage at the zero-cross of the second derivative of the total probe current. Other methods, such as the *method of tangents*, estimation from the position of the maximum of the second derivative [25] or from the probe voltage corresponding to the floating potential [18] etc. are less accurate and not commonly used.

Errors in the determination of the plasma potential by means of this method are related to the phenomena at the probe surface. Among those the change of the work function over the probe surface due to impurities on the probe surface, reflection and secondary emission of electrons, bombardment of the probe surface by metastable atoms and photoemission may be mentioned [19, 20]. The described phenomena round the knee of the probe characteristics in the vicinity of the plasma potential and thus the zero-crossing point of the second derivative does not exactly correspond to the plasma potential. In a case in which the collisions play an important role in the collection of charged particles by the probe the effect of rounding the knee of the probe characteristics also occurs. Klagge and Tichý [21] have specified the conditions under which this effect can be neglected (cylindrical probe), i.e., for

$$K_e(K_e+1)\left(K_e + \ln\left(\frac{l_p}{r_p}\right)\right)^{-1} > 1\,, \tag{1.45}$$

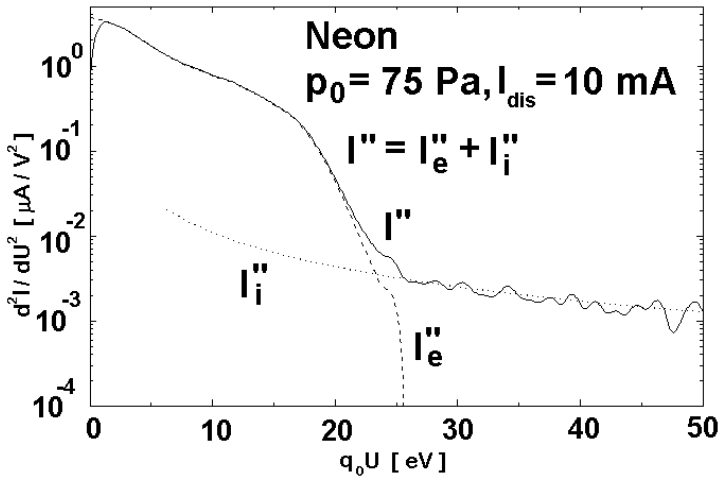

Figure 1.5: Sample of the measured second derivative I''. The relation between the magnitudes of the I''_e and I''_i is shown.

where $K_e = \lambda_e / r_p$ denotes the Knudsen number for electrons.

The second derivative of the electron probe current with respect to the probe potential is usually replaced by the second derivative of the total probe current. This approximation is valid only under the assumption that the ion probe current at higher probe potentials is constant or is a linear function of the probe potential. However, the commonly measured dependence of the positive ion current in a low-temperature non-thermal plasma can be fitted in a better way by the so-called double-logarithmic approximation introduced by Nuhn and Peter [22], i.e. by the relation (for normalized current) $I_i = I_{i0}(1 + \eta_p)^{\kappa}$, where I_{i0} and κ are parameters to be determined from the fit to the experimentally measured dependence. The second derivative of such dependence does not vanish, and sometimes it is a useful practice [23] to correct the second derivative of the total probe current for the second derivative of the positive ion current. An example of the measured second derivative of the total probe current and its decomposition to the second derivative of the electron and of the ion probe current is shown in Fig. 1.5.

The second derivative, necessary for the estimation of the EEDF, either can be directly measured (on-line methods) or computed numerically from the experimental data (off-line methods). Many experimental set-ups for on-line measurement of the second derivative of the total probe current have been developed. They are based on

- making use of the non-linearity of the probe characteristics, i.e. the relation between the *curvature* of the characteristics and second harmonic generation [24], mixing [16], detection of the modulated signal [25] etc.,

- direct analog differentiators using operational amplifiers and sawtooth-like probe voltage [26],

- analog difference amplifiers and stepwise-like probe voltage [27].

The off-line differentiating methods are either based on algorithms of the numerical analysis [28] or on a direct numeric solution of the integral equation 1.9 [29] or on the non-recursive digital filtering of a dependence given as a set of data. The non-recursive digital filter, also called finite impulse response (FIR) filter is applied to a given set of data. It converts the selected data ordinate y_l to a value that is given by a linear combination of itself and of ordinates from its adjacent neighbourhood ($\pm$ m points). The resulting value characterizes the given data in the selected interval around the data point y_l, i.e. it represents the derivative of n^{th} order ($0 \leq n \leq 2m$) at the abscissa corresponding to y_l [30, 31]:

$$y_l^{(n)} \;=\; \frac{1}{h^n} \sum_{i=-m}^{m} c_i y_{l+i}\,. \tag{1.46}$$

Equation 1.46 requires the given data to be equally spaced by h on the abscissa axis. If this condition is not fulfilled the linear interpolation between adjacent points can be used to make the data equally spaced prior to the calculation of $y_l^{(n)}$. It is seen that the value of $y_l^{(n)}$ cannot be obtained at the first m and the last m data points in the given data set. For $n = 0$ Eq. 1.46 represents a weighted smoothing operation. The usual numeric procedures for the differentiation of the experimental data can also be regarded as digital filters since they use formulae analogous to Eq. 1.46.

The most common procedure for differentiation of noisy experimental data is the *sliding polynomial approximation*. This represents the approximation of the selected odd number $M = 2m + 1$ ($m = 1, 2, \dots$) adjacent data points around selected x_l by a second order polynomial $p(x) = a_0 + a_1 x + a_2 x^2$ (for $x_l - mh \leq x \leq x_l + mh$). Hence the second derivative at x_l is $y_l^{(2)}(x_l) = 2a_2$. Since the coefficient a_2 is a weighted sum of the ordinates y_i (for $l - m \leq i \leq l + m$) this method may be regarded as digital filtering where the weights are the filter coefficients $c_i/(h^2)$. Tables of such coefficients are given by Savitzky and Golay [32] and formulae for the evaluation of these filter coefficients in Ref. [33]. Computer programs that make use of this procedure have already been constructed and reported Ref. [34]. However, the variability and the noise-suppression are not always sufficient in the probe diagnostics [35, 36].

Better signal-to-noise-ratio can be obtained if the elements of the digital filter theory are applied. This method consists in a calculation of the second derivative by the method described in the above paragraph and in a subsequent application of the digital filtering on the resulting second derivative data set. The derivative is calculated e.g. by using the 3 or 5 point method, i.e. according to the formulae

$$y_l^{(2)} = \frac{1}{h^2}(y_{l-1} - 2y_l + y_{l+1}) \qquad \text{or} \tag{1.47}$$

$$y_l^{(2)} = \frac{1}{12h^2}(-y_{l-2} + 16y_{l-1} - 30y_l + 16y_{l+1} - y_{l+2})\,. \tag{1.48}$$

The derivatives calculated in this manner feature the quadratic increase of the high noise frequencies in their frequency spectrum, see e.g., Ref. [36]. In order to suppress this noise increase a smoothing filter with an attenuation increasing at higher frequencies steeper than quadratic has to be applied. Such a filter may be obtained by the window function based filter

design [36]. The simplest of such filters is the Hanning filter. It has a beginning stopband attenuation of 44 dB. A design procedure for a smoothing filter with strong increasing noise suppression having a variable beginning stopband attenuation between 27 dB and 80 dB is given in Ref. [36].

Further discussion on the numerical differentiation of probe characteristics is given in Ref. [37]. Here the numerical filtering of the probe data by means of B–spline approximation is applied. Errors that can arise due to the numerical differentiation are treated in Ref. [38]. A further novel smoothing method using the so-called Hayden numerical filtering is described in Ref. [39]. Generally, one has to be careful in the choice of the degree of smoothness in any of the methods mentioned above. Secondary maxima or local deficits of the EEDF due to elementary processes characteristic of the investigated plasma that create or loose electrons in a certain range of energies should not be suppressed. When in doubt whether a particular irregularity on the EEDF is due to the plasma processes or due to noise the best recommendation is to process a set of data with different kinds of differentiating methods and compare the results with theoretical expectations.

In all procedures for the estimation of the second derivative of the probe characteristics the second derivative is estimated not from the infinitesimally small vicinity of the point where the derivative is estimated, but from the finite voltage (energy) interval around this point. This leads to a distortion of the estimated second derivative in comparison with the theoretical one. It has been shown that the estimated second derivative $\overline{I}''(u_p)$ is related to the theoretical one $I''(u_p)$ via convolution with so-called apparatus function $T(u_p - u'_p)$ [40]:

$$\overline{I}''(u_p) = \int_{-\infty}^{+\infty} I''(u'_p) T(u_p - u'_p) du'_p \,. \tag{1.49}$$

A typical course of the apparatus function (case of the second harmonic procedure [41]) is

$$T(u_p - u'_p) = \frac{8}{3\pi} \left(1 - \left(\frac{u_p - u'_p}{a} \right)^2 \right)^{\frac{3}{2}} \,, \tag{1.50}$$

where a is the amplitude of the applied fundamental harmonic. The function $T(u_p - u'_p)$ has non-zero values only for $-1 \leq (u_p - u'_p)/a \leq 1$. Practice has shown that in order to get EEDF's that are close to reality it is a better way to enhance the signal-to-noise ratio of the measured signal from the probe than to try to process numerically the data with a bad signal-to-noise ratio. In any case the deconvolution is not necessary if the peak-to-peak amplitude of the differentiating signal in volts (in the on-line as well as in the off-line case) is less than half the electron temperature expressed in electron-volts, i.e., in our example $2a < k_B T_e/(2q_0)$ [7].

On-line methods have the advantage that the experimenter is at once aware what the signal-to-noise ratio is like and can take measures to increase it if necessary. On the other hand, on-line methods usually do not yield absolute values (unless calibrated which requires additional efforts). However, even if only relative data of the second derivative of the probe characteristics are available it is possible to estimate the electron temperature and/or the electron mean energy.

On the other hand the off-line numeric methods of differentiation yield the absolute values of the second derivative of the probe characteristics. Also, since the experimenter records *merely* the probe characteristics that have a much higher amplitude than the signal of the second derivative, it may seem that usually it takes less effort to set up the experimental system. Yet the noise that may not be visible at first sight on the probe characteristics data can substantially influence the second derivative results. This is easy to comprehend from the fact that the amplitude of the second derivative is usually 2-3 orders of magnitude lower than the amplitude of the probe characteristics. Therefore, as a rule the numeric procedures for differentiating the probe characteristics require probe data of comparatively very good signal-to-noise ratio.

1.5 Probe diagnostics of anisotropic plasmas

All discharge plasmas are to a larger or lesser degree anisotropic. It is possible to make the direction-resolved diagnostics of the electron velocity distribution function (EVDF) with the aid of a planar probe. The normal to the probe plane must be adjustable in different angles θ to the preferred direction (e.g. current flow). It is possible to make the analysis of the probe data acquired in different angles to the preferred direction under the assumption that the EVDF is symmetrical along the preferred direction. In such a case one can expand the EVDF into a series of spherical (Legendre) polynomials with the angle θ as a parameter. In general the expansion has the form

$$f(w_x, w_y, w_z) \;=\; \sum_k f_k(w) P_k(\cos\theta)\;. \tag{1.51}$$

The first three coefficients of the expansion are given by $P_0 = 1$, $P_1 = \cos\theta$, and $P_2 = \frac{3}{2}(\cos^2\theta - 1)$. In these relations θ represents the angle between the preferred direction and the instantaneous velocity $\vec{w}$.

Substituting the expansion 1.51 of the EVDF into the general formula 1.4 for the probe current we obtain

$$I_{p_e} \;=\; -q_0 n_e \int dA_s \int_{w_{x1}}^{w_{x2}} \int_{w_{y1}}^{w_{y2}} \int_{w_{z1}}^{w_{z2}} w_z \sum_k f_k(w) P_k(\cos\theta) dw_x dw_z dw_z\;. \tag{1.52}$$

Due to the rotational symmetry of the problem in question all surface area components dA_s having the same orientation to the anisotropy component of the EVDF should carry the same current. Therefore we can integrate over dA_s to get A_s. Then equation 1.52 can be written in spherical coordinates

$$I_{p_e} = -q_0 n_e A_s \int_{w_1^*}^{\infty} \int_0^{2\pi} \int_0^{\arccos\theta^*} w^3 \sum_k f_k(w) P_k(\cos\theta(\vartheta,\varphi,\Phi)) \cos\vartheta d\vartheta d\varphi dw \tag{1.53}$$

where Φ is the angle between the surface normal and the anisotropy component, and w_1^* and θ^* are the integration limits for the electrons that fall on the probe surface. Differentiating this expression twice with respect to u_p we obtain

$$I''_{p_e\Phi} \;=\; I''_{p_e}(f_0, f_1, f_2, \Phi)\;. \tag{1.54}$$

By measuring the second derivative of the probe characteristics with respect to the probe voltage in three different orientations ($0^\circ, 90^\circ, 180^\circ$) relative to the preferred direction we obtain a set of three equations from which we can determine the first three components in the expansion. The exact formulae were developed by Mesentsev et al. who obtained the following relations [42]:

1. for the electron density:

$$n_e = \left(\frac{1}{3}\right)(2m_e)^{1/2} q_0^{-3/2} A_p^{-1} \int_0^\infty u_p^{1/2} (I''_{p_e 0} + 4I''_{p_e 90} + I''_{p_e 180}) du_p \,, \tag{1.55}$$

2. for the isotropic part of the EVDF:

$$f_0(q_0 u_p) = \left(\frac{1}{3}\right)(2m_e)^{1/2} q_0^{-5/2} n_e^{-1} A_p^{-1} u_p^{1/2} (I''_{p_e 0} + 4I''_{p_e 90} + I''_{p_e 180}) \,, \tag{1.56}$$

3. for the first-order anisotropy of the EVDF:

$$\begin{aligned} f_1(q_0 u_p) &= (2m_e)^{1/2} q_0^{-5/2} n_e^{-1} A_p^{-1} u_p^{1/2} g_1(q_0 u_p) \,, \\ \text{where} \quad g_1(q_0 u_p) &= G_1 + (2q_0 u_p)^{-1} \int_{q_0 u_p}^\infty G_1 d\varepsilon \,, \\ G_1 &= (I''_{p_e 0} \; - \; I''_{p_e 180}) \\ \text{and} \quad \varepsilon &= q_0 u_p \,, \end{aligned} \tag{1.57}$$

4. for the second-order anisotropy of the EVDF:

$$\begin{aligned} f_2(q_0 u_p) &= \left(\frac{2}{3}\right)(2m_e)^{1/2} q_0^{-5/2} n_e^{-1} A_p^{-1} u_p^{1/2} g_2(q_0 u_p) \,, \\ \text{where} \quad g_2(q_0 u_p) &= G_2 + \left(\frac{3}{2}\right)(q_0 u_p)^{-3/2} \int_{q_0 u_p}^\infty \varepsilon^{1/2} G_2 d\varepsilon \\ \text{and} \quad G_2 &= (I''_{p_e 0} - 2I''_{p_e 90} + I''_{p_e 180}) \,. \end{aligned} \tag{1.58}$$

1.6 Probe diagnostics under non-collision-free conditions

The collisionless OML model has been found satisfactory by experimenters for the electron collection by the probe over a comparatively wide range of experimental conditions. However, the positive ion current was underestimated in this model, and this leads to an overestimation of the positive ion density with respect to the electron density when determined from the same probe characteristics even at conditions when the plasma could be assumed as quasi-neutral. This has been found in non-thermal discharge plasmas, see e.g., Ref. [43], as well as in thermal afterglow plasmas [44]. Moreover the Bernstein–Rabinowitz [3] and the Laframboise [4] theory predict that the ion saturation current for the orbital motion limited conditions (OML) should be independent of the Debye number ξ_p, if the probe potential is constant. A comparison of the theoretical and experimental results has shown that in contrary to the

Bernstein–Rabinowitz [3] and Laframboise [4] theory the ion saturation current depends on the Debye number ξ_p at orbital motion limited (OML) conditions and that its magnitude is larger than the theoretically predicted one.

Experimental results obtained by several authors [44, 45, 46] have been summarized by Smith and Plumb [44]. They demonstrated that the ion density n_i determined by the ion current I_i may be expressed in terms of the electron density n_e determined by the electron current I_e by the empirical relationship $n_i/n_e \approx (1 + 0.07\sqrt{m_i/m_H})$, where m_H is the proton mass. From the quasi-neutrality of the plasma follows, however, that the electron density n_e should be equal to the positive ion density n_i assuming that no negative ions are present within the plasma. A difference between n_i and n_e has been observed in Ref. [44] even in the flowing afterglow plasma where the condition for the stable space charge sheath $T_i > T_e/2$ (see, e.g., Ref. [47]) is satisfied. The difference between n_i and n_e cannot be explained by an end-effect phenomenon, i.e. transition to a spherical-like sheath configuration [48]. The experimental results obtained in Refs. [44, 45, 46] therefore indicate an inaccuracy in the assumptions of the OML model of the positive ion collection for the used experimental conditions.

It is believed that these discrepancies can be explained, at least at certain simple experimental conditions, if the collisions of positive ions with neutrals in the space charge sheath around the probe are taken into account. Monte Carlo simulations have shown that already a small number of collisions in the sheath can destroy the orbital motion of an ion [49]. Further discussions are therefore devoted to probe theories that take account of the ion-neutral collisions in the sheath around the Langmuir probe. For the characterization of the pressure the Knudsen number $K_i = \lambda_i/r_p$ has been introduced.

The collection of positive ions by the probe under the influence of ion-neutral collisions has been studied for many years; examples of earlier papers on this subject are Refs. [50, 51, 52, 53, 54, 55, 56]. The theories that treat the problem of the positive ion collection by a Langmuir probe under the influence of collisions of ions with neutrals in the probe sheath can be divided into kinetic and continuum theories; such theoretical models are usually called *collision models* or *collision theories*. The kinetic theories aim at the description of the influence of the individual collision processes to the ion collection; the continuum theories use the hydrodynamical description. The kinetic approach can be regarded as more general since it describes the collisionless conditions too while the continuum theories require the supposition of many collisions. The kinetic theories discussed in this review present the effect of collisions in form of a correction to a collisionless ion collection model. Two collisionless models are used: Laframboise's model [4] that includes the classical Langmuir's orbital motion limited model (OML) [1] and the radial motion cold ion approximation model, called ABR-Chen [5, 57]. We shall not present the thin sheath collision models such as *continuum plus free fall theory* [58, 59] since they require higher plasma densities than usually used in plasma-aided technologies.

The collision probe theory of the positive ion as well as of the electron current to a cylindrical (spherical) probe has been presented by Chou, Talbot and Willis [60, 61]. It describes the Langmuir probe characteristics at arbitrary Knudsen numbers $0 \leq K_i = \lambda_i/r_p \leq \infty$. The result of this theory is a reduction of the ion as well as of the electron probe current due to elastic scattering of these particles caused by collisions with neutrals in the probe sheath. The influence of collisions is calculated as a correction F_T to Laframboise's collisionless ion

current i_i^L. This correction was in a shape more suitable for practical calculations presented by Talbot and Chou [60] and by Kirchhoff, Peterson and Talbot [62].

It is to be noted that there were also other kinetic models for the description of the charged particle collection by a Langmuir probe. Bienkowski and Chang [63] found the solution of the Poisson and Boltzmann equation with the collision term for the limiting case $\xi_p \to \infty$ while Wasserstrom et al. [64] only in the limiting case $\eta \to 0$. Both limits can be, however, derived from the Talbot and Chou theory with the same results. Substantially simpler than the Talbot and Chou theory is the procedure employed by Self and Shih [65] that modified the ABR radial model (for spherical probes) [5] by introduction of the *friction term*. The results are presented as dependencies of the normalized ion current at a certain probe voltage on the ξ_p and the ion-neutral collision frequency ν_{in}. For cylindrical probes the same procedure is applied to the ABR-Chen [5, 57] radial model in Ref. [66].

Klagge and Tichý [21] employing the procedure of Ref. [60] carried out a set of numerical calculations of the positive ion current as a function of the Knudsen number K_i at the normalized potential $\eta = \eta_{fl} - 10$. The difference to the original Talbot and Chou paper [60] consisted in the fact that they used the ABR-Chen [5, 57] collisionless current i_i^A in place of i_i^L in the calculation of F_T. The reason was that the model i_i^A describes with reasonable accuracy the experimental results at conditions close to collision-free. The authors used their own analytical approximation for the numerical Chen [57] currents, see section 1.3.2. The exact step-by-step procedure described in Ref. [21] enables to set up a program that directly calculates the correction F_T.

Zakrzewski and Kopiczynski [67] have introduced another model in which, contrasting the Talbot and Chou theory, elastic collisions of ions with neutral particles have two consequences: the destruction of the orbital motion of ions and the elastic scattering of positive ions. The destruction of the orbital motion can lead to an increase of the positive ion current, too. The effect of the orbital motion destruction predominates for lower pressures when the mean free path of positive ions is bigger or comparable to the sheath thickness. The elastic scattering of the positive ions causes a monotonous decrease of the positive ion current and dominates for higher pressures. As a result the current peak appears at a pressure when on the average one collision of an ion with a neutral in the space charge sheath occurs. Similar as in the ABR-Chen and Laframboise theory and in the Talbot et al. theory [60, 61], the ion current in the Zakrzewski and Kopiczynski theory is normalized by Eq. 1.33. The resulting normalized dimensionless ion current i_i to a cylindrical probe then is $i_i = \gamma_1\gamma_2 i_i^L$, where γ_1 describes the rate of increase of ion current due to destruction of orbital motion, and γ_2 corresponds to the rate of reduction of ion current due to scattering. The correction factor F_Z is given by $F_Z = (\gamma_1\gamma_2)^{-1}$. Zakrzewski and Kopiczynski have derived the coefficient γ_1 under the assumption that at the orbital motion-limited conditions the positive ion current collected by a perfectly absorbing probe is saturated and described by the Laframboise theory. This physical argument can be expressed analytically, assuming that the dimensionless ion current at the sheath edge i_i^A is given approximately by the Allen et al. theory [5]. In the collisionless limit only the current i_i^L predicted by Laframboise reaches the probe surface. The current $(i_i^A - i_i^L)$ leaves the sheath due to the orbital motion.

When an orbiting positive ion undergoes a collision with a neutral particle in the space charge sheath it looses energy and is attracted to the probe. An ion on the average makes $X_i = S/\lambda_i$ collisions in the sheath, if we denote the thickness of the sheath by S and the

ion mean free path by λ_i. According to Zakrzewski and Kopiczynski the rate of increase of the positive ion current due to the destruction of the orbital motion by elastic collision is $\gamma_1 = 1 + \left(i_i^A/i_i^L - 1\right)\frac{S}{\lambda_i}$. Kopiczynski [68] determined the thickness of the sheath S on the basis of numerical calculations carried out by Basu and Sen [69]. Zakrzewski and Kopiczynski estimated the corresponding reduction rate of the ion current due to the elastic scattering γ_2 according to Schulz and Brown [70] and Jakubowski [71]. It should be noticed that for a given probe potential γ_1 and γ_2 are functions of ξ_p and K_i.

For a normalized probe potential $\eta_p = -15$ Kopiczynski [68] carried out an extensive numerical calculation of the dependence of the quantity $i_i\xi_p^2$ on the ion Knudsen number K_i, with the Debye number ξ_p as a parameter. David [72] and David et al. [18] extended these calculations towards lower Knudsen numbers K_i occurring in a medium pressure discharge. The comparison of several of the already mentioned theories of the ion current collection by the probe in the transition pressure regime has been done by David [72].

The results of Talbot and Chou and those of Zakrzewski and Kopiczynski are not in contradiction with each other within the region $2 \leq \xi_p \leq 3$. For lower $\xi_p(\xi_p < 2)$ the ion current calculated by using the Zakrzewski and Kopiczynski theory [67, 68] exhibits a well pronounced maximum at $X_i \cong 1$. At higher values of $X_i \gg 1$ the ion current decreases with decreasing K_i more rapidly than the ion current obtained from the theory [60, 61] in which no current peak is observed.

Since the Chou and Talbot theory [60, 61] does not take into account the effect of the probe current increase due to the orbital motion destruction caused by ion collisions with neutrals within the probe sheath, the theory developed by Zakrzewski and Kopiczynski describes the ion collection by a Langmuir probe at OML conditions in the region where not all the ions suffer a collision with a neutral particle within the probe sheath ($X_i < 1$) more precisely than the Talbot and Chou theory. On the other side for a larger number of ion collisions within the sheath ($X_i \gg 1$) the theory developed by Zakrzewski and Kopiczynski is not applicable at OML conditions since it uses for the evaluation of the factor F_Z the formulae which have been derived in [71] under the assumption of only a few ion collisions within the probe sheath. In order to extend the validity of the theory developed by Zakrzewski and Kopiczynski [67, 68] for an arbitrary K_i it was suggested in Ref. [73] to apply the Talbot and Chou theory [60, 61] for the determination of the factor (or its equivalent) describing the effect of scattering of ions due to their collisions with neutrals within the probe sheath. The corresponding expression following the model used by Zakrzewski and Kopiczynski is $i_i = \gamma_1\gamma_2^* i_i^L$, where γ_2^* is the coefficient describing the effect of the ions scattering due to collisions with neutrals within the probe sheath determined from the Talbot and Chou model [60]. The advantage of the new model [73] of the ion collection by a cylindrical Langmuir probe mainly consists in the fact that it is valid for any K_i, i.e. for $0 \leq K_i < \infty$, as long as the condition of the OML regime of the probe is fulfilled ($\xi_p \leq 3$). In contrast to the calculations of the γ_2 factor which have been made by Zakrzewski and Kopiczynski the correction factor γ_2^* depends on the ratio of the electron to ion temperature $\tau = (T_e/T_i)$. It was suggested in Ref. [73] to call this new model the *modified* Talbot and Chou model since it refines the *classical* kinetic Chou and Talbot theory [60, 61]. A comparison of the theory [73] with the Chen-Talbot [21] and with the Zakrzewski-Kopiczynski [67, 68] theory has been made by Kudrna [74]. He calculated also the dependence of the directly measurable quantity $\xi_p^2 i_i$ on K_i with ξ_p as a parameter. Samples of his results are presented in Fig. 1.6. Note that in both figures the ion current

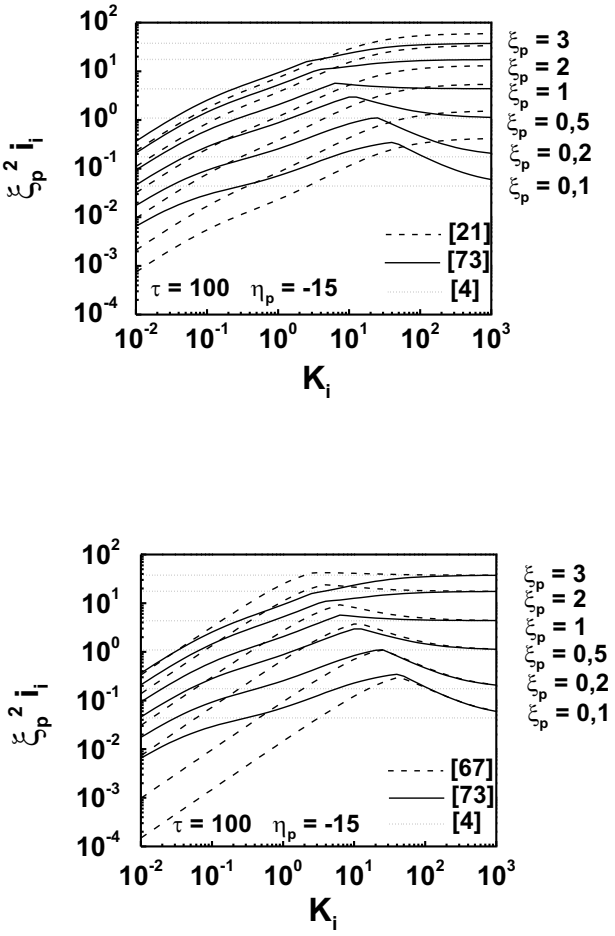

Figure 1.6: (a) Comparison of the Chen-Talbot positive ion current model [21] with the modified Chou-Talbot model [73]. For comparison also the collisionless current model of Laframboise [4] is shown. (b) Comparison of the Zakrzewski-Kopiczynski positive ion current model [67] with the modified Chou-Talbot model [73]. The collisionless current model by Laframboise [4] is also shown.

calculated according to Ref. [73] decreases at lower K_i slower than predicted by the theories of Refs. [21, 67, 68].

Experimental assessment of the applicability of all mentioned collision theories is presented in Ref. [75]. The measurements have been done in a low-pressure flowing afterglow system with a Langmuir probe and downstream mass analysis. Several kinds of ions have been used for this study. Fig. 1.7 presents typical results that have been obtained with rare gas ions Ar^+ in a He carrier gas. The plot shows the numerical values of the ratio of the ion density according to the theory of Ref. [73] to the electron density n_{eVpl} estimated from the

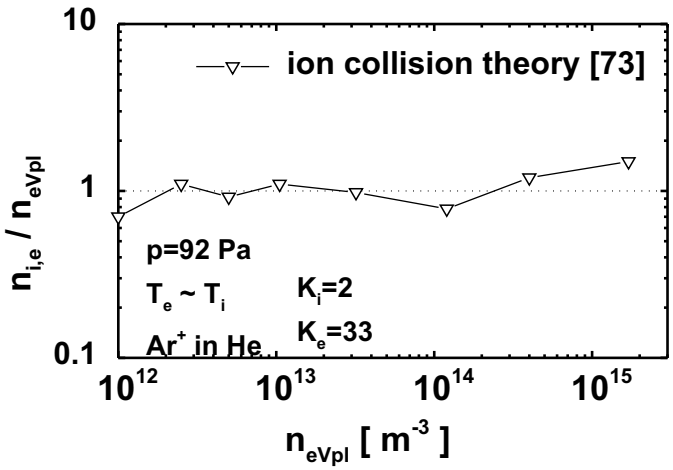

Figure 1.7: The ratio of the ion density evaluated using the theory of Ref. [73] to the electron number density *vs.* electron number density in a flowing afterglow discharge [75].

electron current at the plasma potential *vs.* n_{eVpl}.

The present state of knowledge about the influence of positive ion-neutral collisions in the probe sheath does not, however, allow to name a universally applicable theory that would give satisfactory results in a broad range of experimental conditions; for afterglow conditions the theory of Ref. [73] yields fairly consistent results, for an active plasma (also when the supposition of the Maxwellian EEDF is not quite satisfied) the ABR-Chen theory with the collision correction [21] gives the best agreement with the experiment. More general results might bring the Monte-Carlo simulation of the ion motion in the probe vicinity. First such steps have been made in Ref. [49].

1.7 Langmuir probe in a magnetized plasma

In many technological applications of the low-temperature plasma, for example deposition of thin films or etching of microstructures, a magnetic field is used that confines the plasma and increases the grow/etch rate. The magnetic field in these systems can be either non-homogeneous (usually created by permanent magnets; one example is the planar unbalanced magnetron) or almost homogeneous fields (created by coils) with a strength usually not reaching too high values. When using the Langmuir probe as a diagnostic tool in these systems the question arises up to what limit of the ratio B/p (magnetic field strength to the working pressure; this is a similarity parameter in magnetized plasma) it is possible to use the conventional methods for the evaluation of the basic plasma parameters such as charged particle density and the electron energy distribution function (EEDF) from the Langmuir probe data.

The discussion of the influence of the magnetic field on the probe measurement in the collision-free case can be, in accord with Ref. [76], divided in 4 categories in dependence on

the parameter $\beta = r_p/r_L$ (r_L is the radius of the cyclotron motion of a charged particle): (i) At $\beta \ll 1$, weak B, the influence is small and can be neglected (rare case of technologically interesting applications), (ii) at $\beta \approx 1$, B is still weak, but it is sometimes necessary to introduce small corrections (frequently the case in plasma-aided technologies), (iii) at $\beta > 1$, B is strong, but it is still possible to interpret at least a part of the Langmuir probe characteristics (case of tokamak edge plasma), and (iv) at $\beta \gg 1$, i.e., at very strong B, the probe characteristics are no longer interpretable. From the definition of the parameter β it is evident that β decreases with increasing charged particle velocity and mass; therefore the faster electrons and the ions are less influenced by the magnetic field during their collection by the probe. In other words, the part of the probe characteristics that shows the least distortion due to the magnetic field is that for a very negative probe with respect to the plasma, see, e.g., Refs. [77, 78]. The changes in the probe characteristics therefore are most apparent in the region close to the plasma potential when the probe is applied in a magnetized plasma. The directional movement of charged particles along the magnetic field lines reduces the diffusion of particles in the direction across the field lines. Considering the electron motion which is mostly influenced by the magnetic field, we see that the diffusion coefficient across the field $D_\perp$ reduces to $D_\perp = D_0/(1+\Omega_e^2\tau_{en}^2)$ with $D_0 = v_{th}^2\tau_{en}$, where $\Omega_e = q_0B/m_e, \tau_{en} = 1/\nu_{en}$ and v_{th} are the electron cyclotron frequency, electron-neutral collision time and electron thermal velocity, respectively [79]. If $\Omega_e\tau_{en} \gg 1$ (i.e., a magnetized plasma at low pressures) which holds for most technologically used plasmas, then the expression for $D_\perp$ reduces to $D_\perp \approx v_{th}^2/\Omega_e^2\tau_{en} = r_L^2/\tau_{en}$. In other words in the direction perpendicular to the magnetic field the effective mean free path of electrons is roughly equal to the radius of the cyclotron motion. If the probe draws too much current at probe potentials close to the plasma potential the electrons are absorbed by the probe more rapidly than they can be supplied by diffusion from the distant regions where they are produced. Another effect concerns the change of the effective collecting area of the probe, since the charged particles flow to the probe mostly from the direction of the field lines reducing hence the original probe area to double of its projection to the field direction. Finally, at higher magnetic fields, e.g., in tokamaks, the probe is connected to its reference electrode only by the *current tube*, which reduces the ratio of the reference-electrode-probe surface collecting areas. All three effects then lead to *blurring of the knee* of the probe characteristics near the space potential as seen in Fig. 1.8. When for the data analysis from such an affected probe the conventional methods are used the resulting plasma number density is underestimated, the plasma potential shifted towards probe retarding voltages and the electron temperature deduced from the slope in the electron retarding regime is overestimated. Note that this effect not only depends on the magnetic field strength, but rather on the ratio Ω_e/ν_{en}, or on B/p. The degree of anisotropy of the problem (and hence of the influence to the probe measurements) will therefore depend also on B/p and not on B itself. Thus the assessment of the error caused by the effect of the magnetic field to the probe data and consequently to the accuracy of the estimated plasma parameters is most interesting. Experimental assessment of this effect in weak-to-medium magnetic fields is presented in Refs. [80, 81, 82]. The work is based on the assumption that the influence of the magnetic field on the positive ion collection by the probe is negligible in the range of pressures and of magnetic fields employed. Thus the comparison of the positive ion density estimated from the ion accelerating region of the probe characteristics with the electron density estimated from the electron current at the plasma potential (by a conventional method, i.e. without any cor-

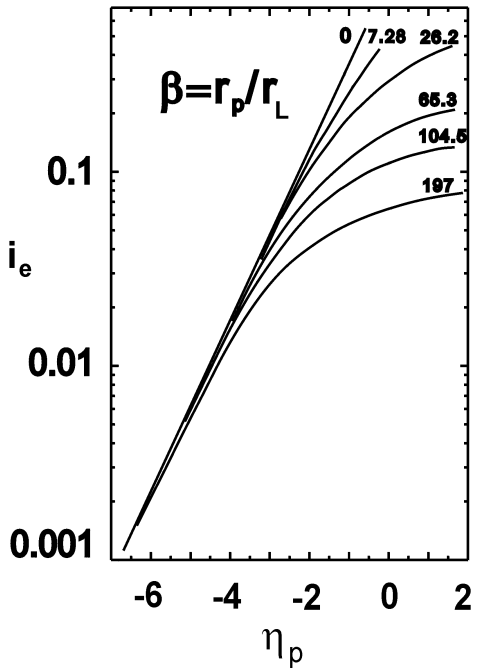

Figure 1.8: The normalized electron probe current *vs.* η_p in dependence on the parameter β for a spherical probe (from Ref. [77]).

rection to the magnetic field) at lower and higher B/p should give an idea of the magnitude of this influence. A sample of experimental results is given in Fig. 1.9. The figure is arranged in a similar manner as Fig. 1.7. It is seen that at higher B/p the electron density estimated from the electron current at the space potential is systematically underestimated, while at low B/p there is an agreement between the estimated values of the ion and electron density; the difference gives a measure for the error due to the magnetic field.

Anisotropy of the plasma in a magnetic field has been studied, e.g., in Refs. [79, 83, 84]. Aikawa [79] used for the determination of plasma anisotropy in a magnetic field two Langmuir probes with their collecting surfaces perpendicular and parallel to the magnetic field.

Ref. [85] deals with the radial distribution of the EEDF in the positive column of a glow discharge in neon in a magnetic field collinear with the electric field. The authors used the *conventional* second harmonics method to obtain the second derivative of the probe characteristics from which they calculated the electron density and the electron mean energy. They found that even at comparatively low values of B/p of the order 10^{-3} T/Pa the magnetic field influences the radial distribution of the mean electron energy in the sense that higher B/p causes the increase of the mean electron energy at larger radii.

Arslanbekov et al. [86] discuss the EEDF measurements by a Langmuir probe at elevated pressures and in a magnetic field. They create an analogy between the effect of an increased pressure and the effect of the magnetic field on the probe characteristics. However in the ana-

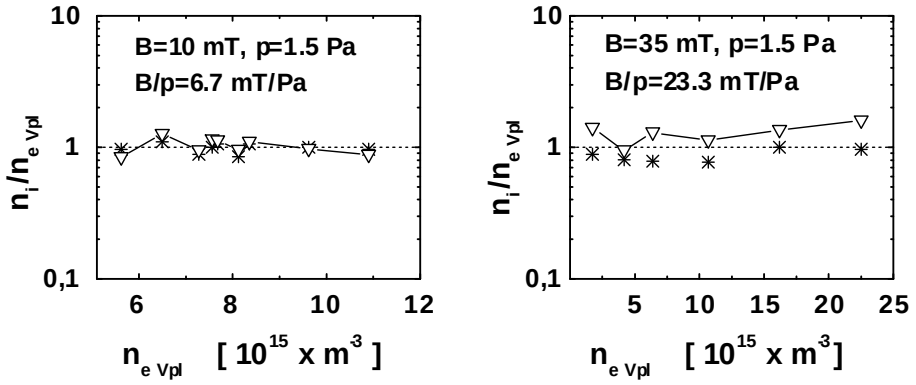

Figure 1.9: Comparison of the relative positive ion (–∇–, theory Ref. [21]) and electron densities (∗, OML theory [1, 4]) estimated from the same probe data at different magnetic fields. *dc* cylindrical magnetron discharge, working gas argon. Reference electron density from the electron current at plasma potential.

lysis of the influence of the magnetic field on the cylindrical probe in a plasma the case of a thin sheath is assumed and hence this work is not directly applicable to the low temperature discharge plasma of technological interest since in such a case the sheath thickness is usually large or comparable to the probe radius. Measurements of the EEDF in the cylindrical magnetron discharge have recently been published in Refs. [87] and [88].

1.8 Space and time resolved Langmuir probe method

1.8.1 Space resolved Langmuir probe measurements

In the case that the plasma is spatially inhomogeneous it is possible to use a probe that is movable along the path of interest, e.g., radially in case of a study of the radial plasma density and electron temperature distribution in a cylindrical discharge tube. The spatial resolution is given by λ_D or by the probe dimension, whichever is bigger. Therefore it is important that the probe dimension should be smaller than the characteristic length of the investigated spatial change. This means that along the probe dimension the plasma parameters should not change considerably. Since the minimum dimension of the Langmuir probe is limited mainly by the dimension of its holder and therefore cannot be easily made smaller than some tenths of a mm, it is almost impossible to study reliably by probes spatial changes of plasma parameters, where the characteristic length is smaller than a few mm (e.g., in narrow plasma jets). Much better spatial resolution can, however, be achieved, if the plasma parameters do not change in all directions in the same manner. In case of cylindrical symmetry, e.g., where the characteristic dimension of change in longitudinal direction is much larger than in the radial one, a thin cylindrical Langmuir probe positioned perpendicularly to the radial direction can

yield a spatial resolution down to some hundred microns.

Most common mechanisms for the movement of the probe in the plasma vessel are based on the *screw-and-nut* principle. The thread, however, should be made sufficiently lose in order to enable the outgasing of the system by baking without the danger of seizing the mechanism afterwards (stub acme screw thread). The transfer of the rotational movement into the plasma vessel is made either magnetically or by using the bellow type rotational transfer (cats tail). The simplest mechanism for moving the probe is a ferromagnetic slug inside the diamagnetic stainless steel or glass tube that is moved by an external (electro-)magnet. The electric lead is made either by a spiral-like wire permanently connected to the probe and the vacuum feedthrough or by a sliding contact.

1.8.2 Time resolved Langmuir probe measurements

Often it is necessary to investigate a plasma that changes in time. Famous are the studies of the variations of the EEDF in ionization waves (moving striations) [89, 90] or in a stationary afterglow [44]. In addition there are many studies using probes for studying plasma in single shot systems, such as tokamaks [91]. Last but not least there are many technologically important applications, where plasmas are generated by means of alternating current (*ac*) or radiofrequency (*rf*) power.

The approach to the problem differs depending on the possibility to make the studied changes of plasma parameters periodic in time with a reasonably short period (at least several Hz). Examples of systems, where the periodicity is realizable, are the mentioned studies of stationary afterglow or of ionization waves, but also *ac* or *rf* generated plasmas. Since the Langmuir probe technique relies upon the formation of a space charge sheath around the probe, its time resolution cannot be higher than the ion plasma frequency, $\omega_{pi} = \sqrt{\frac{q_0^2 n_i}{\varepsilon_0 m_i}}$. If the frequency of plasma variations (e.g., in case of *rf* generated plasmas) is higher than ω_{pi}, only measurements of time-averaged values of plasma parameters are possible by the Langmuir probe. Another interesting frequency is the electron plasma frequency, $\omega_{pe} = \sqrt{\frac{q_0^2 n_e}{\varepsilon_0 m_e}}$. With $n_i \approx n_e = 10^{16}$ m^{-3} we get $\omega_{pe} \approx 1$ GHz, and $\omega_{pi} \approx 3.16$ MHz (for argon). In the assessment of the different working regimes of the probe diagnostics in a time-dependent discharge plasma we restrict ourselves to the case that the plasma is excited by the periodically changing electric field. For the discussion of the relations in such a discharge plasma the detailed knowledge of the complex time response of the electron velocity distribution function in dependence on the frequency of the applied electric field is of highest importance. For weakly ionized plasmas where the Coulomb electron-electron collisions can be neglected the calculations already have been made [92]. The results presented in this work show that the time response of the electron kinetics is given by the ratio of the field frequency to the collision frequencies for the electron momentum (ν_i) and the electron energy (ν_ε) dissipation. Systematic investigations of the case when the Coulomb interactions cannot be neglected are to our knowledge not yet available. In the following discussion we therefore shall use the simplified discussion as it is known from classic books on probe technique [93].

There are 5 regions of operation for Langmuir probes as far as the frequency of plasma generation or plasma changes is concerned:

- $\omega \ll \omega_{pi}$ The ions and electrons are in equilibrium with the superimposed periodically varying electric field. The steady ion as well as the electron current increases due to the *rectification effect* of the non-linear probe characteristics. This incremental increase is independent of the frequency. Also harmonics of ion and electron currents are generated due to the non-linearity of the probe characteristics. Time resolved measurements of plasma parameters are possible. This range of frequencies is typical for low frequency plasma oscillations such as ionization waves, periodically switched discharge etc.

- $\omega \approx \omega_{pi}$ The electrons are in equilibrium with the oscillating electric field. The period of oscillations is comparable to the transit time of ions through the space charge sheath and therefore a small resonance peak in the incremental increase in the steady ion current is observed. Since the resonance effects are difficult to assess it is not recommendable to make probe measurements in this frequency range. This frequency range can be entered when studying the frequency dependence of PECVD technologies, i.e., when the plasma is generated not by a single frequency power *rf* generator, but by a small power signal generator followed by a power amplifier.

- $\omega_{pi} < \omega \ll \omega_{pe}$ The electrons are in equilibrium with the oscillating electric field whereas the ions are not. The incremental increase of electron current remains the same as in the previous two cases, the one of the ion current vanishes. Harmonics of the electron current are generated in the same manner as in the previous cases, those of the ion current are zero. Probe measurements of time-averaged values of plasma parameters are possible provided that the *rf* voltage component between the probe and the plasma is removed. This frequency range is typical for single frequency *rf* discharges (13.56 MHz, 27.12 MHz).

- $\omega \approx \omega_{pe}$ The period of oscillations is comparable to an electron's transit time through the sheath. Therefore a small resonance peak in the incremental increase in the steady electron current is observed. Since the resonance effects are difficult to assess it is not recommendable to do probe measurements in this frequency range. This range of frequencies is not typical for any plasma of technological interest.

- $\omega > \omega_{pe}$ Neither ions nor electrons are able to respond to the oscillating electric field. There is neither incremental increase nor harmonics generation of the steady probe current. The probe measurements can be done in a normal way, i.e., as in a *dc* plasma, provided that the *rf* pick-up does not interfere with sensitive current measuring input of the probe set-up. This range of frequencies is typical for magnetron generated microwave plasmas (2.45 GHz).

The case of periodic changes with $\omega < \omega_{pi}$, where the time resolved measurements can be done, the case of $\omega_{pi} < \omega \ll \omega_{pe}$, where it is possible to measure the time-averaged values of plasma parameters and their relevance to single shot experiments, will be discussed separately.

1.8.2.1 Time resolved probe measurements in periodically changing plasmas at $\omega < \omega_{pi}$

Earlier studies made use of an electronic gate which allowed the passing of the signal from the probe to the signal processing system only for a short time period that was synchronized

with the plasma process under study. Gates were constructed differently, either the probe was attached to the experiment permanently [89, 90] and the probe current was sampled or the gate connected directly the bias to the probe [94, 95], i.e., for the remainder of the time period the probe was floating. The first arrangement avoids the transitional effects that arise by application of the square-wave-like voltage to the probe (for discussion on this effect see, e.g., Refs. [96, 97, 98, 99, 100]), the other one avoids the over-current to the probe if there exists a large change of plasma potential along the studied time period, e.g., when measuring in the periodically switched discharge. Recent application of time-resolved probe measurements in stationary afterglow aimed at estimation of recombination rates of H_3^+ and D_3^+ ions with electrons is given in [101, 102]. Technologically interesting examples present the investigations of the plasma in high-power pulsed magnetron [103, 104, 105, 106] or plasma jet operated in pulsed regime [107].

Most of up-to-date equipment uses the multichannel scaler (either factory made, or in the shape of an add-on card to a personal computer) in order to record the probe current continuously and in synchronism with the plasma periodicity. The modern devices have a time resolution around 1-2 μs per channel. By recording many time dependencies of the probe current at different probe voltages a 3-D matrix of current values at different voltages and times can be formed in a computer memory from which it is easy to construct the probe characteristics in dependence on time by swapping the parameter (voltage) and variable (time) [108, 109]. In order to avoid the destruction of the probe due to the excess current care must be taken to protect the probe if a large change of the plasma potential along the studied time period can be expected [110, 111]. Time-resolved probe measurements in time varying plasma with the frequency 100 kHz [112], and even up to 400 kHz [113], have been reported.

1.8.2.2 Probe measurements of time-averaged plasma parameters at $\omega_{pi} < \omega \ll \omega_{pe}$

There is a permanent interest to study the time-averaged plasma parameters in plasmas generated by an *rf* single frequency generator that operates most often at 13.56 MHz. The incremental increase of the electron probe current in this frequency range degrades the probe characteristics in a sizeable manner making the probe measurements of even just simple plasma parameters such as the floating potential quite useless. However, if a provision is made to remove the *ac* bias voltage component which arises between the plasma and the probe in *rf* generated plasmas the additional electron incremental current can be made negligibly small and decent probe measurements are possible. To remove the *ac* component between the plasma and the probe means to *ac* decouple the probe from the *dc* current measuring circuit and let the probe swing in phase with the plasma potential oscillations. Decoupling is usually done for the generator frequency and its second and eventually also third harmonics by using the parallel LC resonant circuits tuned to the appropriate frequencies (see Fig. 1.10). These decoupling circuits must be located in closest vicinity to the probe in order to avoid any parasitic capacitance of the probe lead to ground. A closer analysis [26] showed that at 13.56 MHz and $T_e \approx$ 1eV any parasitic capacitance of the probe against ground bigger than approximately 10^{-2} pF can significantly distort the measured probe characteristics. The tuning of the filters is often influenced by stray capacitances when the probe is inserted into a metallic plasma reactor. For this reason some authors tried to place the actual tuned filter outside the vacuum chamber and call their probe a *tuned probe* [114].

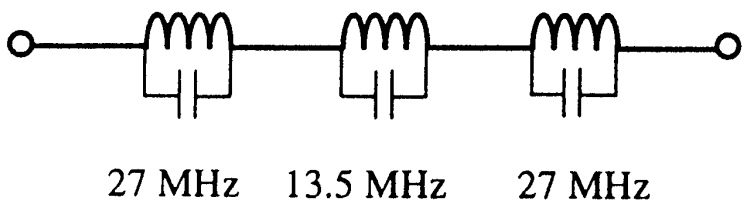

Figure 1.10: Passive LC filters [26].

Instead of the tuned filter the use of the low-pass broadband filter is also possible. Such filters may be constructed of RC elements, i.e. of the resistor in series with the probe together with the parasitic capacitance [115]. In this case the voltage drop on the series resistor must be accounted for. Attempts of using LC broadband filters also have been made [116]. This method uses the resistive impedance of ferrite core chokes. In other words, the choke wound on a low cut-off frequency ferrite core presents high resistance at high frequency while keeping negligible resistance for *dc* current. Therefore it is not necessary to take the voltage drop on the choke(s) into account.

A similar effect as with the decoupling can be achieved by driving the probe by the same voltage waveform as is the waveform of the plasma potential at the probe position. This is a technique used to minimize the capacitance of the inner conductor against ground in a triaxial cable when the internal shield is driven by the amplified voltage of the inner conductor [117]. The realization of this technique is, however, not quite simple, since the plasma potential waveform is not exactly known. Two clones of this technique exist, the drive by the voltage from an external *rf* generator [118] and by the voltage from an additional probe that is positioned close to the measuring one [119, 120]. This additional probe is sometimes isolated from the plasma by a glass tube and is called *capacitive probe* [121]. The *ac* voltage between the plasma and the probe can be minimized by minimizing the plasma potential changes at the probe position, i.e. by symmetric drive of the parallel-plane-electrodes plasma reactor and by positioning the probe in the plane of symmetry between the planar electrodes [26]. A comparison of the passive and the active compensation are presented in Ref. [122]. It is interesting to note that, assuming a Maxwellian distribution and sinusoidal plasma-potential oscillation, electron temperature can be obtained with acceptable error from the *rf* uncompensated probe data; see [123] and the references therein.

A useful modification of the probe method in *rf* plasma presents Ref. [124]. Here the authors measure in the 13.56 MHz *rf* discharge the time-dependence of the *ac* current to the probe in dependence on the *dc* probe bias. From this total current they eliminate the electron component by determining and subsequently subtracting the ion current component and the current component corresponding to the displacement current. From the electron current component they were able to calculate the second derivative with respect to the probe voltage and obtained therefore the EEDF in dependence on the time over the *rf* period. They detected the changes in the tail of the EEDF along the *rf* period as predicted by Winkler et al. [92]. Ref. [124] presents therefore the only (up to our knowledge) time-resolved measurements of the EEDF with the time resolution better than that given by $1/\omega_{pi}$.

1.8.2.3 Time resolved probe measurements in single-shot experiments

In single-shot systems, e.g., in the Langmuir probe studies of the scrape-off layer (plasma in the limiter shadow) of tokamaks the whole probe characteristics have to be acquired during a time which is much shorter than the characteristic time of the change of plasma parameters. The probe voltage is generated either as a sawtooth-like voltage or (simpler) as a sinusoidal voltage with an appropriate period. Care must be taken to measure only the *true* probe current and not the complex (capacitive, displacement) current components that arise due to parasitic capacitances of the probe. If the capacitive current cannot be directly avoided (e.g. due to the indispensable long probe leads) the bridge probe circuit is recommended. The frequency of the probe bias change must fulfill the condition $\omega < \omega_{pi}$. The plasma density in the limiter shadow of tokamaks is generally much higher than 10^{16} m^{-3} therefore also the ω_{pi} is higher and the admissible bias frequency ranges up to several hundreds of kHz. During the stationary phase of a tokamak discharge which lasts up to several seconds it is therefore possible to record several probe characteristics [125].

1.9 Probe diagnostic of chemically active plasmas

During the deposition of conducting and non-conducting layers in a plasma environment the probe diagnostic becomes more complicated. The reason for this consists in the fact that the similar layer as is intended to cover the substrate is deposited both on the probe and on the reference electrode. Generally, the probe surface contamination changes the work function resulting in a deformation of the probe characteristics and/or in hysteresis [126, 127]. If the layer is conducting it helps to centre the probe wire in the insulating holder in such a way that it does not touch the holder walls (see Fig. 1.11). In the case of a non-conducting layer several

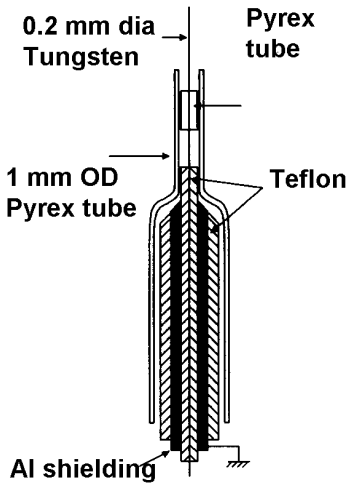

Figure 1.11: Langmuir probe for the use in chemically active plasmas (from Ref. [39]).

approaches have been developed.

- The film is regarded as a series resistance to the probe. Such model has been developed, e.g., in Refs. [128, 129]. This model is simple but its application can be questionable in some cases.

- The film from the probe surface is removed either by periodic ion bombardment of the probe surface and measuring with a short sweep time [130, 131] or by its direct [7, 129, 132] or indirect [133, 134] continuous heating. The heating has the advantage that it prevents the formation of the non-conducting layers, however, the probe construction is more complicated. Further, the heated probe can be usually operated also as the emissive probe that enables easy estimation of the plasma potential [135]. The directly heated probe can also be heated periodically: only prior to the actual measurement. Smart way is to heat the probe using ac (or half-wave ac) power and sample the probe current only when the heating current/voltage reaches zero, see e.g. [136]. This eliminates the uncertainty of the probe bias due to the voltage drop along the probe wire during heating. Examples of use of the emissive probe in the technological magnetron operating in pulsed regime can be found in [137, 138].

- If the conductive reactor wall is used as a reference for a single probe in plasma-chemical environment, the layer on the reference electrode can complicate the measurements, too [139, 140]. If this happens the application of the so-called triple probe method may help [141, 142]. This method uses a floating system of 3 probes, and hence is independent of a reference electrode. The three probes can also be heated thus preventing the layer deposition (see Fig. 1.12). An application of such a probe system is described in Ref. [143].

- A probe that works on another principle is used. One example is the *rf* probe. It makes use of the change of the plasma impedance with the plasma parameters (density, collision frequency). The plasma impedance can be measured directly by means of a vector impedance meter [144]. Alternatively, assuming some simplifications, the conductive part of the plasma impedance can be measured by a bridge circuit [145]. Further, the plasma oscillation probe uses an interesting principle [146]. A beam of electrons injected

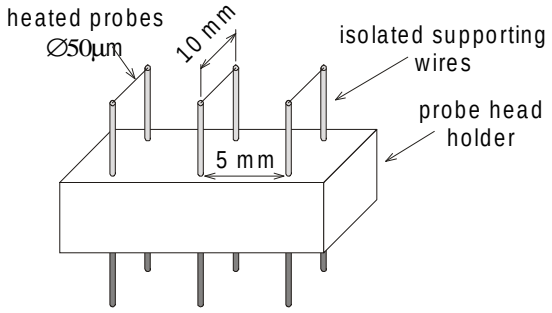

Figure 1.12: Triple heated probe.

into a plasma by a suitably biased hot filament generates plasma oscillations with the plasma frequency ω_{pe} (see section 1.8.2). This frequency can be detected by a small wire-antenna (probe) and measured by a high-frequency spectrum analyzer. Since it is directly coupled to the electron density the knowledge of the plasma frequency means that the plasma density is known, too. Finally, let us mention a novel electrostatic probe method for ion flux measurements [147]. A flat probe is biased by a square-wave-modulated *rf* voltage via a capacitor. During each *rf* voltage pulse the negative *dc* self-bias is generated on the probe. This *dc* bias is then discharged by means of a positive ion flux coming from the plasma. Since this ion current is almost independent of the probe voltage the change of the probe voltage is almost linear, and from its time-derivative it is possible to calculate the ion flux. This method is almost independent of the thickness of the layer on the probe; however, for the method to work properly it is necessary to have a large flat probe (in Ref. [147] the diameter of the probe was 50 mm).

Since in many technological applications oxygen is added to the plasma gas the negative oxygen (mainly atomic) ions can present a problem in probe measurements. Accurate measurements of the negative ion density can only be done with the mass-spectrometer. However, for smaller oxygen percentage in the working gas mixture rough assessment of negative oxygen ions concentration can be done using simple Langmuir probe; the method is based on the comparison of probe characteristics measured with and without oxygen adition at otherwise the same experimental conditions, see Ref. [148, 149]. Further discussion on applications of Langmuir probes in a plasma-chemical environment can be found, e.g., in Refs. [150, 151].

1.10 Double probe technique

When a voltage is applied between two small electrodes immersed in plasma a current flows, and the current-voltage characteristics resemble the ion current part of the single probe characteristics in both polarities of the applied voltage (see Fig. 1.13). In fact the single probe technique obeys the same laws, only one of the electrodes has a much larger surface area than the other one. Therefore we speak of a double probe method only, if the surface areas of both electrodes are small and not very different from each other. The advantage of the double probe

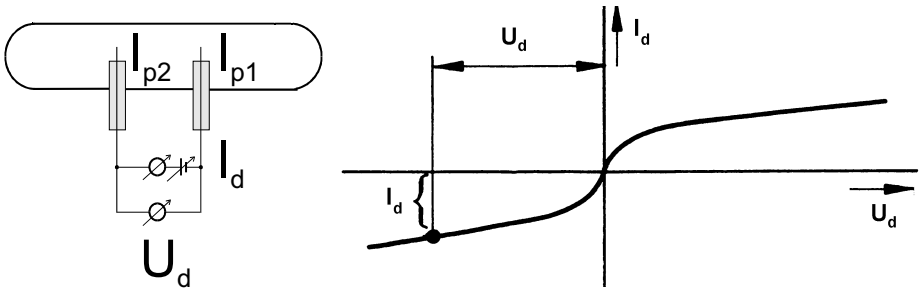

(a) (b)

Figure 1.13: (a) Basic double probe circuit. (b) Typical double probe characteristics.

method is that it does not need the large reference electrode and therefore can be applied in electrode-less (*rf* generated) plasma. The double probe technique is usually applied to measure the electric field in a discharge plasma, but it can also be applied to determine the electron temperature and, at certain experimental conditions, the plasma density.

A usual arrangement in the double probe technique places both probes close to each other so that it is possible to assume that the plasma parameters are the same at both probe positions. Here the words *close* and *small* relate to the characteristic dimension of the change of plasma parameters as discussed in chapter 1.8. If, moreover, both the probes have the same shape and the same surface collecting area, the resulting current-voltage characteristic is centre-symmetrical with respect to the point of zero current.

Just the double probe theory that was originally presented by Johnson and Malter will shortly be described [152]. The suppositions of this theory are the same as that of the Langmuir theory; mainly that the charged particles do not undertake collisions neither with themselves nor with the neutrals in the space charge sheath around the probes. The double probe technique for the electron temperature determination in the middle and higher pressure plasma when the collisions of charged particles with neutrals start to be important has been studied for various plasma conditions by Bradley and Matthews [153], Kirchhoff et al. [154], Klagge and Tichý [21], and Chang and Laframboise [155]. Since the total current drawn by the double probe system from the plasma is zero (the system is floating) it is evident that the current, carried to one probe by particles of a certain charge must be compensated by the current of the second probe due to carriers of the opposite charge. Denoting the first and second probe by the subscripts 1 and 2, respectively, we can write down the following equations based on Kirchhoff's laws:

$$I_{pe1} + I_{pi1} = -(I_{pe2} + I_{pi2}) = I_d \qquad 1^{\text{st}} \text{ Kirchoff law} \tag{1.59}$$

$$U_1 = U_2 + U_d \qquad 2^{\text{nd}} \text{ Kirchhoff law} \tag{1.60}$$

where

$$I_{pe1} = I_{pe1}(U_1) \quad \text{and} \quad I_{pi1} = I_{pi1}(U_1)$$
$$I_{pe2} = I_{pe2}(U_2) \quad \text{and} \quad I_{pi2} = I_{pi2}(U_2)\,.$$

Here $U_{1,2}$ denotes the probe voltage with respect to the space potential, and U_d is the voltage between the two probes. In case of a Maxwellian EVDF it is possible to use the following expression for the electron probe current to the first probe:

$$I_{pe1} = I_{pe}(U_1 = 0)\, \exp\left(-\frac{q_0 U_1}{k_B T_e}\right)\,; \tag{1.61}$$

a similar expression is valid for the second probe. The current in the double probe circuit then is given by:

$$\begin{aligned} I_d(U_d) &= I_{pi1}(U_1) + I_{pe1}(U_1 = 0)\, \exp\left(-\frac{q_0 U_1}{k_B T_e}\right) \\ -I_d(U_d) &= I_{pi2}(U_2) + I_{pe2}(U_2 = 0)\, \exp\left(-\frac{q_0 U_2}{k_B T_e}\right)\,. \end{aligned} \tag{1.62}$$

If we differentiate this double probe characteristics with respect to U_d and take into account that $(dU_d/dU)_{fl} = 2$, then we obtain the expression for the electron temperature firstly derived by Johnson and Malter [152]:

$$\frac{k_B T_e}{q_0} = \left[2 \left(\frac{dI_d}{dU_d} \right)_{fl} - \frac{1}{2} \left(\frac{dI_{pi1}}{dU} + \frac{dI_{pi2}}{dU} \right)_{fl} \right]^{-1} \times \frac{2(I_{pi1})_{fl}(I_{pi2})_{fl}}{(I_{pi1})_{fl} + (I_{pi2})_{fl}} \,. \quad (1.63)$$

Here $(I_{pi1,2})_{fl}$ denotes the extrapolated dependence of the ion current on $U_d = 0$. A modification of this procedure is based on the estimation of the so-called Γ-function, $\Gamma = I_{e1}/I_{e2}$, where the electron temperature T_e is determined from the slope of the dependence $\ln(\Gamma)$ *vs.* U_d

$$\ln(\Gamma) = -\frac{q_0 U_d}{k_B T_e} + \ln\left(\frac{A_1}{A_2}\right) , \quad (1.64)$$

where A_1 and A_2 are the surface collecting areas of the first and second probe, respectively. The great advantage of this method is its insensitivity to the effect of collisions in the space charge sheath around the probe. It has been shown that for $K_i \to 0$ the error of this method does not exceed 15% [21]. Therefore (for the purpose of estimating T_e) it is sometimes advantageous to convert the single probe characteristics to those of the double probe [18]. The procedure is based on the determination of the voltage difference U_{d1} between the two points on the single probe characteristics which correspond to the same absolute value of the chosen probe current I_{d1} but with opposite signs; by choosing I_{d1} from 0 to the maximum ion probe current we obtain the dependence I_{d1} *vs.* U_{d1} that corresponds to one half of the double probe characteristics. The second half is centre-symmetrical with respect to the origin of U_d.

The double probe technique can also be used for the plasma density estimation provided that the model of the positive ion collection by the probe which is suitable for the particular experimental conditions can be applied. A fairly general model has been derived in Ref. [156].

Acknowledgements

This work is a part of the research plan MSM 0021620834 that is financed by the Ministry of Education, Youth and Sports of the Czech Republic.

References

[1] I. Langmuir, H.M. Mott-Smith, Gen. Elec. Rev. **26** (1923) 731.

[2] D. Bohm, E.H.S. Burhop, H.S.W. Massey, The Characteristics of Electrical Discharges in Magnetic Fields, A. Guthrie, R.K. Wakerling (Eds.), McGraw-Hill: New York (1949), p. 77.

[3] I.B. Bernstein, J.N. Rabinowitz, Phys. Fluids **2** (1959) 112.

[4] J.G. Laframboise, Univ. of Toronto, Institute for Aerospace Studies (UTIAS), Report **100** (1966).

[5] J.E. Allen, R.L.F. Boyd, P. Reynolds, Proc. Phys. Soc. B **70** (1957) 297.

[6] A.A. Sonin, AIAA Journal **4** (1966) 1588.

[7] S. Klagge, DSc Thesis, University of Greifswald, Germany (1988).

[8] B.M. Annaratone, M.W. Allen, J.E. Allen, J. Phys. D: Appl. Phys. **25** (1992) 417.

[9] J.E. Allen, Physica Scripta **4** (1992) 497.

[10] J.E. Allen, Plasma Sources Sci. Technol. **4** (1995) 234.

[11] C.M.C. Nairn, B.M. Annaratone, J.E. Allen, Plasma Sources Sci. Technol. **4** (1995) 416.

[12] J.E. Allen, B.M. Annaratone, U. de Angelis, J. Plasma Phys. **63** (2000) 299.

[13] J. Rohmann, S. Klagge, Contrib. Plasma Phys. **33** (1993) 111.

[14] J.I. Fernández Palop, J. Ballesteros, V. Colomer, M.A. Hernández, J. Phys. D: Appl. Phys. **29** (1996) 2832.

[15] M.J. Druyvesteyn, Z. Physik **64** (1930) 781.

[16] S.C.M. Luijendijk, J. Van Eck, Physica **36** (1967) 49.

[17] D. Herrmann, S. Klagge, Beitr. Plasmaphysik **12** (1972) 17.

[18] P. David, M. Šícha, M. Tichý, T. Kopiczynski, Z. Zakrzewski, Contrib. Plasma Phys. **30** (1990) 167.

[19] S. Aisberg, 3rd Symp. Engineering Aspects of Magnetohydrodynamics (1963), p.89.

[20] W. Seifert, D. Johanning, H.R. Lehmann, N. Bankov, Beitr. Plasmaphysik **26** (1986) 237.

[21] S. Klagge, M. Tichý, Czech. J. Phys. B **35** (1985) 988.

[22] B. Nuhn, G. Peter, Proc. XIII. ICPIG Berlin (1977), p. 999.

[23] M. Šícha, Czech. J. Phys. B **29** (1979) 640.

[24] G.R. Branner, E.M. Friar, G. Medicus, Rev. Sci. Instr. **34** (1963) 231.

[25] N.A. Vorobjeva, J.M. Kagan, V.M. Milenin, Zhurnal tekhnicheskoi fiziki (J. Tech. Phys. USSR) **34** (1964) 2079.

[26] V.A. Godyak, R.B. Piejak, B.M. Alexandrovich, Plasma Sources Sci. Technol. **1** (1992) 36.

[27] B. Saggau, Z. Angew. Physik **32** (1972) 324.

[28] W.H. Press, S.A. Teukolsky, W.T. Wetterling, B.P. Flannery, Numerical Recipes in C (The art of scientific computing), Cambridge University Press (1988, 1992).

[29] L.M. Volkova, A.M. Devyatov, G.A. Kralkina, N.N. Sedov, M.A. Sherif, Vestnik Mosk. Univ. (fizika, astronomija) **16** (1957) 502.

[30] A.V. Oppenheim, R.W. Schafer, Discrete-Time Signal Processing, Prentice-Hall (1989).

[31] J.F. Kaiser, W.A. Reed, Rev. Sci. Instr. **48** (1977) 1447.

[32] A. Savitzky, M.J.E. Golay, Anal. Chem. **36** (1964) 1627.

[33] H. Madden, Anal. Chem. **50** (1978) 1383.

[34] M. Tichý, P. Kudrna, J.F. Behnke, C. Csambal, S. Klagge, Journal de Physique IV **7** (1997) C4-397.

[35] M. Hannemann, Greifswalder Physikalische Hefte **6** (1983) 145; PhD Thesis, University of Greifswald, Germany (1991).

[36] M. Hannemann, INP-Report VII, Institute for Low-Temperature Plasma Physics, Greifswald (1995).

[37] D. Trunec, Contrib. Plasma Phys. **32** (1992) 523.

[38] M. Tichý, M. Šícha, J. Bok, S. Pfau, Czech. J. Phys. B **37** (1987) 179.

[39] J.I. Fernández Palop, J. Ballesteros, V. Colomer, M.A. Hernández, Rev. Sci. Instr. **66** (1995) 4625.

[40] H. Amemyia, J.Appl.Phys. **15** (1976) 1767.

[41] V.I. Demidov, N.B. Kolokolov, Zhurnal tekhnicheskoi fiziki (J. Tech. Phys. USSR) **51** (1981) 888.

[42] A.P. Mesentsev, A.S. Mustafaev, V.L. Fedorov, Zhurnal tekhnicheskoi fiziki (J. Tech. Phys. USSR) **55** (1985) 544; V.L. Fedorov, Zhurnal tekhnicheskoi fiziki (J. Tech. Phys. USSR) **55** (1985) 926.

[43] M.B. Hopkins, W.B. Graham, Rev. Sci. Instr. **57** (1986) 2210.

[44] D. Smith, I.C. Plumb, J. Phys. D: Appl. Phys. **6** (1973) 196.

[45] L. Tonks, I. Langmuir, Phys. Rev. **34** (1929) 876.

[46] J.F. Shaeffer, PhD Thesis, University of St. Louis (1971).

[47] F.F. Chen, in Plasma Diagnostics Techniques, R.H. Huddelstone, S.L. Leonard (Eds.), Academic Press: New York, London (1965).

[48] J. Virmont, Proc. IX. ICPIG, Bucharest, Contrib. papers (1969), p. 609.

[49] D.Trunec, P. Španěl, D. Smith, Contrib. Plasma Phys. **35** (1995) 203.

[50] C.V. Goodall, D. Smith, Plasma Physics **10** (1968) 249.

[51] C.V. Goodall, B. Polychronopoulos, Planet. Space Sci. **22** (1974) 1585.

[52] M.G. Dunn, J.A. Lordi, AIAA Journal **7** (1969) 1458.

[53] M.G. Dunn, J.A. Lordi, AIAA Journal **8** (1970) 1077.

[54] R.A. Johnson, P.C.T. DeBoer, AIAA Journal **10** (1972) 664.

[55] J.A. Thornton, AIAA Journal **9** (1971) 342.

[56] V.M. Zakharova, J.M. Kagan, K.S. Mustafin, V.I. Perel, Sov. Phys. Tech. Phys. **5** (1960) 411.

[57] F.F. Chen, Plasma Phys. **7** (1965) 47.

[58] J.D. Swift, Proc. Phys. Soc. **79** (1969) 697.

[59] J.F. Waymouth, Phys. Fluids **7** (1964) 1843.

[60] L. Talbot, Y. S. Chou, Rarefied Gas Dynamics, Academic Press (1966), p. 1723.

[61] Y.S. Chou, L. Talbot, D.R. Willis, Phys. Fluids **9** (1966) 2150.

[62] R.H. Kirchhoff, E.W. Peterson, L. Talbot, AIAA Journal **9** (1971) 1686.

[63] K.G. Bienkowski, K.W. Chang, Phys. Fluids **11** (1968) 784.

[64] E. Wasserstrom, C.H. Su, R.F. Probstein, Phys. Fluids **8** (1965) 56.

[65] S.A. Self, C.H. Shih, Phys. Fluids **11** (1968) 1532.

[66] C.H. Shih, E. Levi, AIAA Journal **9** (1971) 1673, AIAA Journal **9** (1971) 2417.

[67] Z. Zakrzewski, T. Kopiczynski, Plasma Physics **16** (1974) 1195.

[68] T. Kopiczynski, PhD Thesis, IMP PAN, Institute of Fluid-Flow Machines, Polish Academy of Sciences, Gdansk, Poland (1977).

[69] J. Basu, C. Sen, Japan J. Appl. Phys. **12** (1973) 1081.

[70] G.J. Schulz, S.C. Brown, Phys. Rev. **98** (1955) 1642.

[71] A.K. Jakubowski, AIAA Journal **8** (1972) 988.

[72] P. David, CSc Thesis, Faculty of Mathematics and Physics, Charles University Prague (1985).

[73] M. Tichý, M. Šícha, P. David, T. David, Contrib. Plasma Phys. **34** (1994) 59.

[74] P. Kudrna, PhD thesis, Charles University Prague, Czech Republic (1996).

[75] O. Chudáček, P. Kudrna, J. Glosík, M. Šícha, M. Tichý, Contrib. Plasma Phys. **35** (1995) 503.

[76] P.M. Chung, L. Talbot, K.J. Touryan, Electrical Probes in Stationary and Flowing Plasmas, Theory and Application, Springer-Verlag: Berlin, Heidelberg, New York (1975).

[77] J.R. Sanmartin, Phys. Fluids **13** (1970) 103.

[78] J.G. Laframboise, J. Rubinstein, Phys. Fluids **19** (1976) 1900.

[79] H. Aikawa, J. Phys. Soc. Japan **40** (1976) 1741.

[80] E. Passoth, P. Kudrna, C. Csambal, J.F. Behnke, M. Tichý, V. Helbig, J. Phys. D: Appl. Phys. **30** (1997) 1763.

[81] P. Kudrna, E. Passoth, Contrib. Plasma Phys. **37** (1997) 417.

[82] P. Kudrna, O. Chudáček, M. Šícha, M. Tichý, E. Passoth, J.F. Behnke, Proc. XXII. ICPIG, Hoboken, K.H. Becker, W.E. Carr, E.E. Kunhardt (Eds.), Contributed Papers, Vol. 2 (1995), p. 185.

[83] J.C. Blancod, K.S. Golovanievski, T.P. Kravchov, Proceedings X. ICPIG, Oxford (1971), p. 25.

[84] J.G. Brown, A.B. Compher, K.W. Ehlers, D.F. Hopkins, W.B. Kunkel, P.S. Rostler, Plasma Phys. **13** (1971) 47.

[85] Z. Zakrzewski, T. Kopiczynski, M. Lubanski, Czech. J. Phys. B **30** (1980) 1167.

[86] R.R. Arslanbekov, N.A. Khromov, A.A. Kudryavtsev, Plasma Sources Sci. Technol. **3** (1994) 528.

[87] J.F. Behnke, E. Passoth, C. Csambal, M. Tichý, P. Kudrna, D. Trunec, A. Brablec, Czech. J. Phys. B **49** (1999) 483.

[88] E. Passoth, J.F. Behnke, C. Csambal, M. Tichý, P. Kudrna, Ju.B. Golubovskii, I.A. Porokhova, J. Phys. D: Appl. Phys. **32** (1999) 2655.

[89] S.W. Rayment, N.D. Twiddy, Brit. J. Appl. Phys. **2** (1969) 1747.

[90] M. Šícha, V. Veselý, V. Řezáčová, M. Tichý, M. Drouet, Z. Zakrzewski, Czech. J. Phys B **21** (1971) 62.

[91] J. Dvořáček, L. Kryška, J. Stöckel, F. Žáček, M. Šícha, M. Tichý, V. Veselý, Czech. J. Phys. B **40** (1990) 678.

[92] R. Winkler, J. Wilhelm, A. Hess, Annalen der Physik **42** (1985) 537.

[93] J.D. Swift, M.J.R. Schwar, Electrical Probes for Plasma Diagnostics, Iliffe Books: London (1970).

[94] A.B. Blagoev, N.B. Kolokolov, V.M. Milenin, Zhurnal tekhnicheskoi fiziki (J. Tech. Phys. USSR) **42** (1972) 1701.

[95] A.B. Blagoev, J.M. Kagan, N.B. Kolokolov, R.I. Lyaguschenko, Zhurnal tekhnicheskoi fiziki (J. Tech. Phys. USSR) **44** (1974) 333.

[96] D. Kamke, H.J. Rose, Z. Physik **145** (1956) 83.

[97] P.R. Smy, J.R. Greig, J. Phys. D **1** (1968) 351.

[98] R.W. Carlson, T. Okuda, H.J. Oskam, Physica **30** (1964) 182; T. Okuda, R.W. Carlson, H.J. Oskam, Physica **30** (1964) 193; H.J. Oskam, R.W. Carlson, T. Okuda, Physica **30** (1964) 375.

[99] K.-D. Weltmann, PhD thesis, University of Greifswald, Germany (1993).

[100] T. Bräuer, PhD thesis, University of Greifswald, Germany (1997).

[101] R. Plašil, J. Glosík, V. Poterya, P. Kudrna, J. Rusz, M. Tichý, A. Pysanenko, International J. Mass Spectrom., Review, **218** (2002) 105.

[102] V. Poterya, J. Glosík, R. Plašil, M. Tichý, P. Kudrna, A.Pysanenko, Phys. Rev. Lett. **88** (2002) 044802-1.

[103] Th. Welzel, Th. Dunger, H. Kupfer, and F. Richter, J. Appl. Phys. **96** (2004) 6994.

[104] Th. Welzel, Th. Dunger, St. Welzel, H. Kupfer, F. Richter, Surf. Coat. Technol. **200** (2005) 630.

[105] A Belkind, A. Freilich, J. Lopez, Z. Zhao, W. Zhu, and K. Becker, New Journal of Physics **7** (2005) 90.

[106] J. Alami, J.T. Gudmundsson, J. Bohlmark, J. Birch and U. Helmersson, Plasma Sources Sci. Technol. **14** (2005) 525.

[107] J. Olejníček, Z. Hubička, P. Virostko, A. Deyneka, L. Jastrabík, P. Adámek, M. Šícha, M. Tichý, H. Šíchová, Czech. J. Phys. **56** (2006) Suppl. B (accepted).

[108] A.G. Dean, D. Smith, I. Plumb, J. Phys. E **5** (1972) 776.

[109] B.M. Wunderer, J. Phys. E **8** (1975) 938.

[110] T. Bräuer, S. Gortschakow, D. Loffhagen, S. Pfau and R. Winkler, J. Phys. D: Appl. Phys. **30** (1997) 3223.

[111] T. Bindemann, M. Tichý, J.F. Behnke, H. Deutsch, Rev. Sci. Instr. **69** (1998) 2037.

[112] M.B. Hopkins, C.A. Anderson, W.G. Graham, Europhysics Letters **8** (1989) 141.

[113] K.R. Stalder, C.A. Anderson, A.A. Mullan, W.G. Graham, J. Appl. Phys. **72** (1992) 1290.

[114] Ajit P. Paranpje, James P. McVittie, Sidney A. Self, J. Appl. Phys. **67** (1990) 6718.

[115] U. Flender, B.H. Nguyen Thi, K. Wiesemann, N.A. Khromov, N.B. Kolokolov, Plasma Sources Sci. Technol. **5** (1996) 61.

[116] P. Špatenka, V. Brunnhofer, Meas. Sci. Technol. **7** (1996) 1065.

[117] U. Tietze, Ch. Schenk, Halbleiter-Schaltungstechnik, Springer-Verlag: Berlin, Heidelberg, New York (1980).

[118] N.St.J. Braithwaite, N.M.P. Benjamin, J.E. Allen, J. Phys. E **20** (1987) 1046.

[119] P.A. Chatterton, J.A. Rees, W.L. Wu, K. Al-Assadi, Vacuum **42** (1991) 489.

[120] W. Kasper, Proc. XXII. ICPIG, Hoboken, K.H. Becker, W.E. Carr, E.E. Kunhardt (Eds.), Contributed Papers, Vol. 2 (1995), p. 171.

[121] M. Sugawara, J. Ichihashi, Y. Kobayashi, Proc. XVIII. ICPIG, Swansea, W. Terry Williams (Ed.), **4** (1987) 830.

[122] B.M. Annaratone, N.St.J. Braithwaite, Meas. Sci. Technol. **2** (1991) 795.

[123] L. Oksuz, F. Sobern, and A. R. Ellingboe, J. Appl. Phys. **99** (2006) 013304.

[124] R.B. Turkot, Jr., D.N. Ruzic, J. Appl. Phys. **73** (1993) 2173.

[125] M. Hron, J. Stöckel, L. Kryška, J. Horáček, Proc. IAEA Technical Committee Meeting on Research Using Small Tokamaks, Prague (1996), p. 54.

[126] R. D'Arcy, J. Phys. D: Appl. Phys. **7** (1974) 1391.

[127] E.P. Szusczewicz, J.C. Holmes, J. Appl. Phys. **46** (1975) 5134.

[128] S. Klagge, Beitr. Plasmaphys. **15** (1975) 309.

[129] J. Kalčík, Czech. J. Phys. **45** (1995) 241.

[130] P. Špatenka, R. Studený, H. Suhr, Meas. Sci. Technol. **3** (1992) 704.

[131] K. Shimizu, K. Yano, H. Oyama, H. Kokai, Proc. ISPC-9, Bari (1989), p. 831.

[132] Y. Kobayashi, T. Ohte, M. Katoh, M. Sugawara, Trans. IEE of Japan **109-A** (1989) 69.

[133] M. Niionomi, K. Yanagihara, ACS Symp. **108** (1979) 87.

[134] C. Winkler, D. Strele, S. Tscholl, R. Schrittwieser, Proc. 12^{th} SAPP, Liptovský Ján (Slovakia), J.D. Skalný, M. Černák (Eds.), p. 121 (1999).

[135] E.Y. Wang, N. Hershkowitz, T. Intrator, C. Forest, Rev. Sci. Instr. **57** (1986) 2425.

[136] J.J. Schuss, R.R. Parker, J. Appl. Phys. **45** (1974) 4778.

[137] J.W. Bradley, S. Thompson and Y. Aranda Gonzalvo, Plasma Sources Sci. Technol. **10** (2001) 490.

[138] J.W. Bradley, S.K. Karkari and A. Vetushka, Plasma Sources Sci. Technol. **13** (2004) 189.

[139] P. Špatenka, H. Suhr, Plasma Chemistry and Plasma Processing **13** (1993) 555.

[140] P. Špatenka, Z. Beneš, Frontiers in Low Temperature Plasma Diagnostic, Book of Papers, Bad Honnef, Germany (1997), p. 227.

[141] S. Chen, T. Sekiguchi, J. Appl. Phys. **36** (1965) 2363.

[142] T. Okuda, K. Yamamoto, J. Appl. Phys. **31** (1960) 158.

[143] P. Špatenka, H.-J. Endres, J. Krumeich, R.W. Cook, Surface and Coating Technology **116–119** (1999) 1228.

[144] E.A. Mosburg, R.C. Abelson, J.R. Abelson, J. Appl. Phys. **54** (1983) 4916.

[145] R. Johnsen, Rev. Sci. Instr. **57** (1986) 428.

[146] A. Brockhaus, A. Schwabedissen, Ch. Soll, J. Engemann, Proc. Frontiers in Low Temperature Plasma Diagnostic III, Saillon (Switzerland, 1999), p. 89.

[147] N.St.J. Braithwaite, J.P. Booth, G. Cunge, Plasma Sources Sci. Technol. **5** (1996) 677.

[148] M. Shindo, S. Hiejema, Y. Ueda, S. Kawakami, N. Ishii, Y. Kawai, Surf. and Coat. Technol. **116-119** (1999) 1065.

[149] M. Shindo, Y. Kawai, Surf. and Coat. Technol. **142-144** (2001) 355.

[150] U. Flender, K. Wiesemann, Plasma Chem. Plasma Process. **15** (1995) 123.

[151] H. Sabadil, S. Klagge, M. Kammayer, Plasma Chem. Plasma Process. **8** (1988) 425.

[152] E.O. Johnson, L. Malter, Phys. Rev. **80** (1950) 58.

[153] D. Bradley, K.J. Matthews, Phys. Fluids **6** (1963) 1479.

[154] R.H. Kirchhoff, E.W. Peterson, L. Talbot, AIAA Journal **9** (1971) 1686.

[155] J.S. Chang, J.G. Laframboise, Phys. Fluids **19** (1976) 25.

[156] M. Šícha, M. Tichý, V. Hrachová, P. David, T. David, J. Touš, Contrib. Plasma Phys. **34** (1994) 51.